

ABSTRACT

Title of Thesis: MYSIDS IN NEARSHORE FOOD WEBS OF
CHESAPEAKE BAY TRIBUTARIES

Lael Donyé Collins, Master of Science, 2025

Thesis Directed By: Dr. Michael Wilberg, and Marine Estuarine
Environmental Sciences

Mysids, particularly *Neomysis americana* and *Americamysis* spp., are abundant crustaceans in the nearshore Chesapeake Bay that are important for connecting the microscopic and macroscopic portions of food webs. However, the effects of fish predation on mysid communities and prey of mysids are not well understood in these habitats. Our objectives were to 1) estimate the effect of predation of mysids by fishes in a shallow nearshore habitat of the Patuxent River in Chesapeake Bay and 2) determine the diet of mysids *in situ* in the St. Marys and Patuxent rivers. For objective 1, we conducted nighttime fish sampling using a 30×1.2 m beach seine, and mysids were sampled during the day using a 500 μm -mesh epibenthic sled approximately weekly during August–September, 2023. Consumption of mysids was quantified by enumerating mysids found in the stomachs of each species of finfish and comparing estimates of consumption to estimates of mysid abundance. Only *Americamysis* spp. were observed during the study period, and estimated abundance fluctuated across sampling days. Estimated daily consumption varied among fish species, and the aggregate daily predation mortality rate of the local mysid population was estimated to be 1.1% d^{-1} . We used DNA metabarcoding of the

stomach contents of mysids sampled using an epibenthic sled and zooplankton nets from the St. Marys and Patuxent rivers to characterize mysids' diets *in situ*. Dual-indexed amplicon-based high throughput sequencing was used to generate meta barcode libraries from the small subunit gene (18S) from pooled mysid stomachs. A small portion (0.18%) of our metabarcoding sequences were identified as non-mysid taxa, including copepods, fungi, macroalgae, microalgae, protists, segmented worms, tunicates, terrestrial plants, hydrozoans, and fish. Length of consumer mysid and time of sampling best predicted abundance of putative prey sequences. There was not a significant relationship between the length of consumer mysids and the putative prey they consumed. The results of this thesis are useful for building our knowledge of the Chesapeake Bay food web and of trophic niche of mysids.

MYSIDS IN FOOD WEBS OF CHESAPEAKE BAY TRIBUTARIES

by

Lael Donyé Collins

Thesis submitted to the Faculty of the Graduate School of the
University of Maryland, College Park, in partial fulfillment
of the requirements for the degree of
Master of Science
2025

Advisory Committee:

Professor Michael Wilberg, UMCES CBL, Chair

Associate Professor Ryan Woodland, UMCES CBL

Principal Investigator Katrina Lohan, Smithsonian Environmental
Research Center

© Copyright by
Lael Donyé Collins
2025

Acknowledgements

I would like to thank the National Science Foundation for funding most of this project and providing the opportunity for me to take on this endeavor. Financial support for materials and travel was also provided by the St. Marys River Watershed Association, Chesapeake Biological Laboratory Graduate Education Committee, and University of Maryland Jacob K. Goldhaber Travel Grant. I would also like to thank the Smithsonian Institution Fellowship Program accepting me as a 2024 Fellow, aiding in the completion of my research.

I would like to thank my primary advisor, Michael Wilberg, and committee members, Ryan Woodland, and Katrina Lohan. Mike, without you seeing my potential as a prospective intern, absolutely none of this would have been possible. You've had confidence in my ability to become a scientist even before I did, which I am so grateful for. Ryan, I know your mentorship in how to conduct a study will take me far into my career. Thank you so much for always providing opportunities for me to be hands on in the field and learn new techniques and applications. Katrina, I appreciate your patience and going out on a limb for someone with so little genetic experience. My time talking with you and working in your lab provided me with an entirely new scope on where my career could go in the future. Thank you to my whole committee for the faith you have put in me, not only to succeed in this project, but to move forward in life being the best scientist I can be.

I thank the UMCES and CBL community, for being like a second family to me, making Maryland like a home away from home. Specifically, I would like to thank members of the Wilberg Lab: Samara (my very first mentor), Sam, Maya, Kaitlynn, Ray, Madison, and Sarah. Without you all, I would be clueless to navigating the scientific world (or real world for that matter), as I was a real newbie upon starting this project. Additionally, I would like to express

my appreciation towards the Woodland lab members: Theresa, Nina, Matt, Kyle, Pauline, and the Woodland family. When it wasn't readily helping with middle-of-the-night sampling, or staying up during week-long research cruises, it was the forging of friendships and sharing of memes that helped me to see this through. Thanks to all of my lab siblings, I'd be helpless without you. To Caroline, my roommate over the course of my thesis, thank you for being a great support system, enduring my unending mysid tangents, and chatting about reality TV during my brain breaks. I want to also thank the members of the Coastal Disease Ecology lab at SERC: Ruth, Maddy, Emma, Calli, and Isabella. You were all so patient and instructive with me learning the ropes during my fellowship and made SERC like a home away from my home away from home. You all have provided so much friendship and guidance over the course of my thesis, making it an experience I will never forget.

Finally, I would like to express my gratitude to my personal friends and family. To my hometown friends, Hope, Lexie, Arielle, Hailey, Tamia, and Aiyana who always stick around even when I am too buried with work to consistently text back. To my dog, Bambam, who's snout gets whiter and whiter every time I go back home but still renews me with energy upon every visit. To my pop-pop who is always eager to hear about the fish we're catching - even when we're just sampling for mysids. To my brother, Langston, who inspires me to be confident in myself. To my dad who always suggests I cook anything I catch. And finally, to my mom who I can always count on, night or day, for words of encouragement or comfort. I couldn't have done this without you.

Table of Contents

Acknowledgements.....	ii
Table of Contents.....	iv
List of Tables.....	vi
List of Figures.....	vii
Chapter 1: Estimated fish predation mortality rates on a nearshore mysid community in the Patuxent River, Maryland.....	1
Introduction.....	1
<i>Mysid Overview</i>	1
<i>Mysid Mortality</i>	2
<i>Mysids in Chesapeake Bay</i>	2
<i>Objectives</i>	3
Methods.....	3
<i>Study Area</i>	3
<i>Mysid Sampling</i>	4
<i>Finfish Sampling</i>	5
<i>Analysis</i>	6
Results.....	8
<i>Mysid Abundance</i>	8
<i>Finfish Abundance</i>	9
<i>Finfish Consumption of Mysids</i>	10
<i>Predation Rates</i>	11
Discussion.....	12
<i>Predation Rates</i>	12
<i>Mysid Densities and Abundances</i>	12
<i>Consumption of Mysids</i>	13
<i>Dissection Findings</i>	14
<i>Preliminary Study</i>	15
<i>General Assumptions</i>	16
Conclusion.....	17
Tables.....	18
Figures.....	21
References.....	28
Chapter 2: Using DNA metabarcoding to characterize mysid diets in the Chesapeake Bay.....	33
Introduction.....	33
<i>Mysid Overview</i>	33
<i>Mysids in Food Webs</i>	33
<i>Mysid Feeding Modes</i>	34
<i>Diet Methodology</i>	34
<i>Mysids in Chesapeake Bay</i>	36
Methods.....	36
<i>Sampling</i>	36
<i>Dissections</i>	37
<i>DNA Metabarcoding and Bioinformatics</i>	38

<i>Analysis</i>	40
Results	45
<i>Post-Sequencing</i>	45
<i>St. Marys River</i>	46
<i>Patuxent River</i>	47
Discussion	49
<i>Mysid Diet Data</i>	49
<i>Comparison of Mysid Diets</i>	50
<i>Mysid Diet Methodology</i>	52
<i>GAM variables</i>	53
<i>Mysid Length and Trophic Levels</i>	55
<i>Parasitism</i>	56
<i>Secondary Prey</i>	56
<i>Mysid Digestion and Evacuation</i>	57
<i>Tag-Jumping</i>	58
<i>General Assumptions</i>	58
Conclusions	59
Tables	60
Figures	64
References	71
Appendix A	82
Tables	82
Figures	94
Supplementary Files	97

List of Tables

Table 1.1: Dates of the mysid survey and seine survey.....	18
Table 1.2: Species of fish caught in the seine survey, the number of each species (Num Spp.), the length ranges for each species, and the mean length of each species. Abbreviations for the fish species are Atlantic croaker (AC), Atlantic needlefish (AN), black drum (BD), halfbeak (HB), Atlantic menhaden (AM), silver perch (SP), southern kingfish (SK), spot (ST), spotted sea trout (SS), weakfish (WF), white perch (WP).....	19
Table 1.3: Summary of stomach contents data of finfish from beach seine sampling in the lower Patuxent River during August-September, 2023. Species of fish (Spp. Fish) that were dissected are listed in the first column, followed by the total number of fish examined (Tot. Fish) and the total number of mysids consumed (Tot Mys.). The proportion (Prop.) of individuals in each species of fish found to have the identified prey item are provided by prey taxa: amphipods (Amp.), fish, insects (Ins.), polychetes (Poly), crabs, foliage (Fol.), shrimp (Shr.), and isopods (Isop.). See Table 1.2 for fish species name abbreviations.....	20
Table 2.1. Unique amplicon sequence variants (ASVs), genus, common name, microalgae type and abundance of the ASV in all samples combined from the St. Marys and Patuxent Rivers. ..	60

List of Figures

Figure 1.1: Study location in the lower Patuxent River, Maryland, U.S.A. with the study area represented by a dashed line (a), an aerial view of the Chesapeake Biological Laboratory (CBL) Research Pier with arrows indicating the locations and directions of epibenthic sled tows (b), and a zoomed in aerial view of the CBL Research Pier with seine sampling areas in red. The orange arrow represents the structured tow parallel to the pier (Pier). The green arrow represents the shallow open water tow (Open). The blue arrow represents the deep water tow (Deep). 21

Figure 1.2: Counts of mysids from each epibenthic sled tow (rows) for each mysid sampling day (columns). Transects are described in Figure 1.1b. Catches of each species are represented by colors: *Americamysis almyra* in brown, *A. bahia* in pink, and *A. bigelowi* in light blue. 22

Figure 1.3: Estimated daily abundance of mysids (solid line), 95% confidence intervals (shaded area), and mean mysid abundance (dashed line) in the lower Patuxent River sampling area. Abundance estimates were calculated using non-parametric bootstrapping. 23

Figure 1.4: Number of fish caught by species in beach seine sampling the in the lower Patuxent River during August–September, 2023. See Table 1.2 for fish species name abbreviations. 24

Figure 1.5: Estimated abundance of fish species that consumed mysids from beach seine samples in the lower Patuxent River during August–September, 2023. The box plots represent results from 10,000 non-parametric bootstrap replicates. The heavy lines indicate the median of the abundance estimates for each species, the boxes indicate the 25th and 75th percentiles, and the whiskers represent 95% confidence intervals. See Table 1.2 for species name abbreviations. 25

Figure 1.6: The mean number of mysids per stomach by fish species from the lower Patuxent River during August-September, 2023. The value of mean mysids per stomach for Atlantic needlefish was 0.012 d^{-1} and 0.053 d^{-1} for spot. See Table 1.2 for species name abbreviations. . 26

Figure 1.7: Estimated daily consumption of mysids (a), daily predation mortality rates (b), and 44-day predation mortality rates (c) by fish species and all species combined (Total) in the lower Patuxent River during August–September, 2023. The definitions of the boxes and whiskers are the same as those in Figure 1.5. See Table 1.2 for species name abbreviations. 27

Figure 2.1. Sampling sites in the St. Marys River and Patuxent River, Maryland. Patuxent Hypoxic is Patuxent Site 2, and Patuxent Normoxic is Patuxent site 5 in the text. St. Marys Fished is St. Marys site 1, and St. Marys Unfished is St. Marys site 2 in the text. 64

Figure 2.2. Logarithm (base 10) of abundance of sequences by sampling site and ASV groups from the a) St. Marys River and b) Patuxent River, Maryland. The sample IDs are on the x-axis. 65

Figure 2.3. Frequency (\log_{10} -scale) of amplicon sequence variants (ASVs) for taxa identified in the a) St. Marys mysid-excluded, b) St. Marys mysid-included, c) Patuxent mysid-excluded, and d) Patuxent mysid-included sequences. The scales of the y-axis are 0–10 for the mysid-excluded sequences, and 0–40 for the mysid-included sequences. ASVs are described in Table 1. 66

Figure 2.4. a) Pearson correlations for binary data of the presence of the ASV groups in the Patuxent River and b) the co-occurrences and co-absences of prey groups. In panel a, the circle color represents the sign of the correlation, with warmer colored circles being negative correlations and cooler colored circles being positive correlations. Circle sizes indicate the strength of the correlations. P-values of each correlation (not corrected for multiple comparisons) are in the lower diagonal matrix. 67

Figure 2.5. a) Pearson correlations for binary data of the presence of the ASV groups in the Patuxent River and b) the co-occurrences and co-absences of prey groups. In panel a, the circle

color represents the sign of the correlation, with warmer colored circles being negative correlations and cooler colored circles being positive correlations. Circle sizes indicate the strength of the correlations. P-values of each correlation (not corrected for multiple comparisons) are in the lower diagonal matrix. 68

Figure 2.6. Estimated generalized additive model relationships between mean mysid length in a sample and length of the young of prey of taxa identified using DNA metabarcoding for a) St. Marys mysid excluded, b) St. Marys mysid included, c) Patuxent mysid-excluded, and d) Patuxent mysid-included samples. The black lines represent the estimated relationships, the black points are the data, and the grey shaded areas are the 95% confidence intervals. 69

Figure 2.7. Proportion of mysid stomach samples with non-mysid taxa identified using DNA metabarcoding for the Patuxent River as a function of length. The predicted presence is represented by the black line with 95% confidence intervals in grey. Points include a random jitter to reduce overlap. 70

Chapter 1: Estimated fish predation mortality rates on a nearshore mysid community in the Patuxent River, Maryland

Introduction

Mysid Overview

Mysids are important links in many aquatic and marine food webs (Dean et al., 2005, Mayor et al. 2017, Oliveira et al., 2023). They are common prey for many fishes and other higher trophic level organisms, and they serve as a connector between the microscopic levels of the food web and larger organisms (Dean et al 2005, Buchheister & Latour 2015, Mayor et al 2017, Mayor & Chigbu 2018, Oliveira et al., 2023). Additionally, mysids are often abundant in aquatic and shallow nearshore estuarine habitats (Dean et al., 2005, Rappé et al., 2011, Mayor et al., 2017, Oliveira et al., 2023), which makes them an important prey source for many juvenile fishes (Dean et al 2005, Ludsin et al., 2009, Rappé et al., 2011, Buchheister & Latour 2015, Oliveira et al., 2023). Similarly, adult fishes also regularly consume mysids, but the effects of fish predation on mysid populations have yet to be well documented (Idhe 2015, Mayor et al., 2017, Mayor & Chigbu 2018, Oliveira et al., 2023). Mysids undergo diel vertical migrations (DVM), moving to deeper waters during the day and higher in the water column at night (Oliveira et al., 2023). Due to their diel vertical migrations, and patchy assemblages, mysids are often difficult to sample, so relatively little is known about mysid population dynamics despite their central role in aquatic food webs (Ribes et al., 1996, Allen 1984, Mayor et al., 2017).

Mysid Mortality

Estimated mortality rates of mysids *in situ* are highly variable, and the mortality due to predation (i.e., predation mortality) has rarely been estimated. Clutter & Thielacker (1971) estimated a median instantaneous mortality of *Metamysidopsis elongata* of 0.04–0.06 d⁻¹ based on the ontogenetic stage and assumed that most of the *M. elongata* natural mortality was due to predation. A study in a Netherlands estuary estimated that mortality rates were 0.009 and 0.012 d⁻¹ for *Neomysis kadiakensis* depending on sex and seasonal cohort, based on field catches and aging (Mees & Hamerlynck 1994). Ikeda (1992) estimated an instantaneous 1.040 yr⁻¹ (0.003 d⁻¹, assuming a 3-yr mysid life span) lifetime average mortality rate for *Meterythropeus microphthalmus* in Toyama Bay, Japan by using an exponential decay model. However, few studies specifically estimate predation mortality of mysids *in situ* despite indirect evidence of predation. For example, Mayor and Chigbu (2018) found that the abundance of *Neomysis americana* and *Americamysis* spp. was negatively correlated with fish abundance in the Maryland coastal bays. Dean et al., (2005) found that decreases in mysid abundance were followed by decreases in zooplanktivorous fish species, also suggesting strong ties between these predator-prey populations.

Mysids in Chesapeake Bay

In the Chesapeake Bay region, there are two prominent genera of mysids, *Neomysis* and *Americamysis* (Mayor & Chigbu 2018). *Neomysis*, represented solely by *N. americana* in the region, is more abundant than *Americamysis bahia* in the nearby Maryland coastal bays during much of the year (Mayor et al., 2017, Mayor & Chigbu 2018). However, *Neomysis americana* is less tolerant to heat and decreases in abundance in late summer, which is when the more southerly distributed *Americamysis* spp. (*A. almyra*, *A. bahia*, and *A. bigelowi*) increase in

relative abundance (Mayor & Chigbu 2018, Quill 2024). Less is known about seasonal patterns in abundance of *Americamysis* spp., but they likely fill a similarly important role in nearshore estuarine food webs for at least part of the year.

Objectives

Given the reported importance of mysids in juvenile fish diets and the lack of information on effects of fish predation on mysids, our objectives were to 1) estimate mysid population density and abundance, 2) quantify consumption of mysids by fish using stomach contents analysis, and 3) estimate predation mortality rates on an assemblage of mysids in a nearshore region of the Chesapeake Bay. We combined field sampling of mysid abundance with estimated predation by fishes to estimate predation mortality rates during late summer to early fall on mysids in the Patuxent River, Maryland.

Methods

Study Area

The study area was in the lower Patuxent River near the Chesapeake Biological Laboratory (CBL) research pier in Solomons, Maryland, USA (Figure 1.1a). The study area is centrally located in Chesapeake Bay, with depths ranging from 0.5 to 3 m. The salinity of this region can range from 8.8 to 18, and water temperature ranges from about 3.3° to 28° C (Wingate & Secor 2008). Benthic habitat in the study area is primarily flat sandy bottom, with a mixture of small rocks, shell hash, and occasional *Rupia maritima* seagrass beds. Areas closer to the research pier were slightly more structured due to the presence of pilings and debris.

For estimating mysid abundance and fish abundance, we used an area of the home range of a white perch (*Morone americana*, 0.11 km²; McGrath et al, 2009). White perch is one of the

larger species of predatory finfish that were caught during sampling for this project, and therefore we assumed that home ranges of mysids and other fish species would be similar to or smaller than the home range of white perch.

Mysid Sampling

We collected mysids weekly with an epibenthic sled during August 17–September 28, 2023 (Table 1.1). The mouth of the net mounted on the sled was 0.38 m wide by 0.16 m high with a mesh size of 1 mm. We towed the sled at a speed of about 0.5 m/sec. We conducted sled tows one day per week, at 1100 on the day, with three tows on each sampling day (Figure 1.1b). The three tows included a diagonal tow from the pier to the shore (~26.1 m), a tow parallel to the pier (~30.7 m), and a third tow near the end of the research pier (~38 m) for swept areas of 9.92, 11.67, and 14.44 m². The tows sampled shallow open-water habitat, shallow structured habitat, and a relatively deeper water habitat that has more structure and submerged aquatic vegetation (*Ruppia maritima*). The first two tows sampled depths between 0.5 and 1 m, while the third tow reached depths of 2.0–2.5 m. Following each tow, the contents of the sled net were gently sieved to remove most of the sediment, then rinsed and transferred to secondary containers in the field. In the lab, the samples were fixed in 8% buffered formalin (v/v) for 1–2 weeks, rinsed and soaked in DI water for 2–3 days, then preserved in 75–80% ethanol for long-term storage. During fixation, the samples were stained with Rose Bengal to aid in separating mysids from inorganic sediment and detritus. We counted mysids from each tow and recorded the counts to be used for abundance and density estimates. We took a subsample of 50 mysids per tow to be used to estimate species proportions for each sampling day. We also recorded the location of the sled tow and the date and time of sampling.

Finfish Sampling

We sampled finfish at night, in an area that is spatially adjacent to the mysid sampling in waters less than 1.5 m deep (Table 1.1). We seined every other week at slack tide. We initially planned to start sampling on August 3, 2023, but poor weather conditions caused the survey to start on August 15, 2023. To make up for the missed sampling day, we sampled on September 18th. We used a 30.0 × 1.2 m beach seine with 6.0 mm mesh (Wingate and Secor 2008). We fully deployed the seine perpendicular from shore and swept in a quarter circle back to shore (Figure 1.1c; Wingate and Secor 2008). The area covered by the seine was primarily sandy and flat, with no debris or seagrass beds. Seining took place at night because few mysids were observed in the stomachs of fish captured during the day in a pilot study in 2022. We conducted two hauls each sampling night, one on each side of the CBL pier. We retained a sample of potential mysid predators caught each week for stomach contents analysis. Potential mysid predators were determined based on the 2022 pilot study and descriptions of mysids in the diet from other studies: spotted sea trout (*Cynoscion nebulosus*), weakfish (*Cynoscion regalis*), silver perch (*Bairdiella chrysoura*), spot (*Leiostomus xanthurus*), Atlantic croaker (*Micropogonias undulatus*), southern kingfish (*Menticirrhus americanus*), black drum (*Pogonias cromis*), Atlantic needlefish (*Strongylura marina*), and white perch (*Morone americana*). Atlantic menhaden (*Brevoortia tyrannus*) and halfbeak (*Hyporhamphus unifasciatus*) are not thought to consume mysids but were kept because they were in a size class of fish that could consume mysids (Table 1.2; Lewis & Peters 1994, Guedes et al., 2024). American gizzard shad (*Dorosoma cepedianum*), bay anchovy (*Anchoa mitchilli*), and Atlantic silversides (*Menidia menidia*) were caught, but not retained because they did not consume mysids in the 2022 pilot study. After capture, we froze the fish at -50 °C to prevent further digestion until dissection.

Prior to dissection, species, total length (mm), and weight (g) were recorded for each fish. We recorded total stomach wet weight, the wet weight of stomach contents, presence-absence of identifiable prey taxa, count and wet weight of mysids. Mysids in the stomach contents were not identified to species due to the degradation of their species-specific features (e.g., telson spinage).

Analysis

Densities of mysids were estimated as number caught, divided by the area sampled by the epibenthic sled tow (Figure 1.1). We calculated the mean density (\underline{n}_m) of mysids across the three epibenthic sled tows for each day. Mysid abundance (N_m) was estimated for each sample date as the product of the study area (A ; 0.11km²) and the mean density,

$$N_m = A\underline{n}_m.$$

This approach provides a minimum estimate because it assumes that the epibenthic sled has a catchability of one for mysids (i.e., all mysids in the tow path are caught).

Abundance of each fish species (N_s) for each night of sampling was estimated as the product of the total study area and the mean density (\underline{n}_s) divided by the seine catchability (q),

$$N_s = A \left(\frac{\underline{n}_s}{q} \right).$$

We assumed that the catchability of the seine was 0.59 based on a depletion experiment that estimated the proportion of total individuals captured on the first seine (R. Woodland unpublished data).

Per capita daily consumption of mysids (m_s) was calculated by dividing the total number of mysids observed in stomachs of a species of fish (m_c) by the number of individuals of that fish species that were examined (n_f),

$$m_s = \frac{m_c}{n_f}.$$

The estimated daily consumption of mysids by each species of fish (M_s) per day was calculated as the product of the estimated abundance of each species of fish and the estimated per capita daily consumption of mysids,

$$M_s = N_s m_s.$$

This approach assumed that the number of mysids found per stomach represented the number consumed in the previous 24 hours (Eggers 1977).

The per capita daily predation mortality rate was calculated as the consumption of mysid by each fish species divided by the estimated mysid abundances.

We used non-parametric bootstrapping to estimate the per capita daily predation mortality rate of mysids and its uncertainty (Efron and Tibshirani 1994). Our bootstrapping approach involved calculating average mysid abundance and the consumption of mysids by each fish species and dividing the estimate of mysid consumption by estimated mysid abundance. Mean mysid abundance was calculated for each sampling day by drawing a sample of six values of mysid density for each day with replacement, and the mean over these six days was calculated for one bootstrap replicate. Similarly, the mean abundance of each fish species was calculated as the mean of five abundance estimates drawn with replacement. The same was done for the daily per capita consumption of mysids by each fish species. Lastly, predation mortality was calculated as the daily consumption of mysids divided by the mysid abundance for each replicate. 10,000 bootstrap replicates were generated, and the mean and 95% confidence intervals of the bootstrap samples were summarized.

Estimated predation mortality over the 44-day study period (T) was also calculated for each fish species and for all fish species combined using the bootstrap samples. The daily

survival of mysids from predation by each species was calculated as one minus the predation mortality rate for each fish species,

$$S_s = 1 - \frac{M_s}{N_m}$$

Cumulative mortality (T_s) over the 44-day study period was calculated as the cumulative survival over 44 days subtracted from one,

$$T_s = (1 - S_s^{44}).$$

This equation was implemented for each bootstrapped sample, to produce 10,000 values for predation mortality for each fish species. Finally, the bootstrap estimates of consumption were summed over fish species to estimate the total number of mysids consumed (M_t) per day and across the 44-day study period,

$$M_t = \sum_s M_s$$

Total predation mortality (T_x) was calculated as the sum of predation mortality by each species for the 44-day study period,

$$T_x = T_{Croaker} + T_{A.Needlefish} + T_{S.Kingfish} + T_{silver\ perch} + T_{spot} + T_{weakfish} + T_{white\ perch}$$

Results

Mysid Abundance

Americamysis was the only genus found in the epibenthic sled samples (Figure 1.2). We identified individuals of three species: *Americamysis bahia*, *Americamysis bigelowi*, and *Americamysis almyra*. Estimated mean mysid densities varied among sites and weeks (Figure A1.1), and there was a significant difference between the densities in the structured, shallow

water habitat compared to the shallow open water and deep tow transects (ANOVA; $p = .002$). More mysids were estimated in the shallow region parallel to the pier (mean density = 76.70 mysids/m²) and the fewest mysids were estimated in the shallow region's open transect (mean density = 6.21 mysids/m²). The deep water transect had a mean density of 9.86 mysids/m². Estimated mean mysid abundance fluctuated over time between 0.66-5.84 million individuals with an average of 3.14 million mysids (Figure 1.3).

Finfish Abundance

We caught 135 fish from 11 species of our potential mysid predators (Figure 1.4; Table A1.1). The total lengths of individual fish ranged from 72 to 565 mm (Table 1.2). Atlantic croaker was the only species caught on each sampling night, but Atlantic needlefish was the most abundant fish in our survey (Table A1.2).

The median estimated abundance of fish species varied between 155–3693 individuals across species (Figure 1.5). Atlantic needlefish had the highest estimated abundance, followed by Atlantic croaker, silver perch, and spot. The abundances for each species besides Atlantic needlefish were relatively small, the median abundance for Atlantic croaker, silver perch, and spot being 373.48, 311.24, and 248.99 individuals. The median estimated abundances for southern kingfish and weakfish were 31.12 and 62.25 individuals. The spread of the abundance estimates was highest for needlefish with 95% of estimates falling between 1105.37 and 3936.65 individuals, and lowest for weakfish between 0 and 84.97 individuals. Individual fish species and mysid abundances were not significantly correlated with one another (Table A1.2).

Finfish Consumption of Mysids

A total of 690 mysids were identified in the stomach contents of seven fish species (Figure 1.6). The mean number of mysids in the fish stomachs varied substantially among species. The mean number of mysids per stomach varied between 1 and 85 d⁻¹ among fish species that consumed mysids (Figure 1.6). Weakfish and white perch had the highest mean number of mysids per stomach at 60–84.80 d⁻¹. The mean number of mysids per stomach were 13.58 d⁻¹ for silver perch and 14 d⁻¹ for southern kingfish. The rest of the fish species had mean numbers of mysids per stomach less than 1.09 d⁻¹. Southern kingfish, weakfish, silver perch had the highest percent positive occurrence of mysids at 100%, 100%, and 90% of the species respectively, but only one fish was sampled for southern kingfish and weakfish (Figure 1.3).

In addition to mysids, the fish stomachs also contained fish, polychaetes, amphipods, isopods, decapod shrimp, brachyuran crabs, plant material, and unidentifiable material (Table 1.3). Insects were only found in Atlantic needlefish stomachs, and crabs were only found in Atlantic croaker stomachs. Isopods were only identified in the stomachs of Atlantic needlefish and Atlantic croaker. Non-mysid shrimp were only in the stomachs of silver perch and southern kingfish. Amphipods were identified in the stomachs of Atlantic croaker, Atlantic needlefish, silver perch, southern kingfish, spot, and white perch. Polychaetes were identified in Atlantic croaker, Atlantic needlefish, black drum, half beak, silver perch, spot, and white perch stomachs. We identified fish in the stomachs of Atlantic croaker, Atlantic needlefish, silver perch, spotted sea trout, and white perch.

The estimated number of mysids consumed by each fish species followed a similar pattern to the average number per stomach (Figure 1.7a). The median estimates of mysid consumption by silver perch (8,229.3 mysids d⁻¹) and white perch (22,366.8 mysids d⁻¹) were

higher than the rest of the fish species combined. The next highest median consumption was weakfish (3,165.1 mysids d⁻¹), southern kingfish (1,477.1 mysids d⁻¹), and Atlantic croaker (685.8 mysids d⁻¹). Atlantic needlefish and spot had the lowest median consumption estimates (52.8 mysids d⁻¹).

Predation Rates

The estimated daily mortality rates of mysids varied among fish species, but the median values were less than 1% d⁻¹ for all species (Figure 1.7b). The daily predation rates followed the same pattern as the consumption values, with the highest median predation mortality rates by silver perch and white perch (0.26% and 0.69% d⁻¹, respectively). Weakfish, southern kingfish, and Atlantic croaker had estimated median predation mortality rates ranging from 0.02 to 0.1% d⁻¹. The Atlantic needlefish and spot predation mortality rates were less than 0.01% d⁻¹. The median predation rate of all the fish species combined was 1.10% d⁻¹ (95% CI -0.40–2.59 d⁻¹). Based on relative variability, the predation mortality rates by white perch were most variable, likely due to them being caught inconsistently (Table A1.3). Over the 44-day study period, the estimated mortality rate of mysids due to fish predation (combined over species) was 37.4% (Figure 1.7c). White perch had the highest mysid predation mortality rate of 26.0% over the 44-day study period. The 44-day predation mortality rates of mysids from the remaining species were: silver perch (10.94%), weakfish (4.18%), southern kingfish (1.99%), Atlantic croaker (0.92%), spot (0.07%), and Atlantic needlefish (0.07%).

Discussion

Predation Rates

We estimated the abundance of a mysid assemblage in the lower Patuxent River during late summer and quantified predation mortality by a community of nearshore fish species. Our study is novel in that we estimated predation mortality on *Americamysis* spp. using abundance and fish stomach contents data. Our median predation mortality rate was 0.011 d^{-1} , which is in the middle of other published mysid mortality rates. Clutter & Thielacker (1971) estimated mortality rates for *M. elongata* in immature and adult stages between $0.04\text{--}0.06\text{ d}^{-1}$, and Mees et al., (1994) estimated mortality rates between 0.009 and 0.012 d^{-1} for *N. integer*. Ikeda estimated a daily instantaneous mortality rate of 0.003 d^{-1} for mysids estimated to live to three years. However, *A. bahia*, a species in our sampling, with life cycles similar to *A. almyra* and *A. bigelowi*, are not expected to survive more than 90 days based on laboratory experiments (Kuhn et al., 2000). Our estimates may differ from those in the literature due to differences in causes of mortality among species, differences in timing of sampling during the year, or differences in estimation methodology. For example, the focus on multiple ontogenetic stages of mysids may be the cause for varying mortality rates. Additionally, most other studies involved a longer period of sampling than our study and used length structure to estimate mortality rates.

Mysid Densities and Abundances

We found the mysid assemblage to be made up of *Americamysis* spp., which agrees with the early fall increase of *Americamysis* spp. in the sampling of Mayor & Chigbu (2017) in Maryland's coastal bays and Quill (2024) in the Patuxent River, that abundance of *Americamysis* spp. increase during autumn. Mysids were more abundant in the shallow waters during August-

September than the deeper site. The shallow, structured habitat had a mean mysid density of 76.70 mysids/m² which was 1–12 times that of the deep water site (6.21 mysids/m²) or shallow open habitat (9.86 mysids/m²). Experimental studies and *in situ* sampling have found mysids may aggregate in structured habitats like reefs, piers, or shellfish beds (Connell 2008, Gergs et al., 2008, Boscarino et al., 2020). Our mysid densities were also lower than that of Allen (1984), who sampled *Americamysis bigelowi* (previously *Mysidopsis bigelowi*), and frequently caught over 100 mysids / m² during 1975–1977 in Hereford Inlet, New Jersey. We only found 100+ mysids per m² in our shallow structured samples, a difference that may be caused by having fewer samples within a smaller time frame (Figure A1.1). Our *Americamysis bahia* densities were higher than those of Mayor et al. (2017), who estimated 0.7 ± 0.4 mysids / m² from 2010 to 2013 in Maryland Coastal Bays. The differences in our densities are likely due to the different locations sampled and the variation in times of year sampled. Our estimated abundances of mysids ranged from 0.66–5.84 million individuals, with peaks on a nearly biweekly basis. The reasoning for this pattern would also require more studies to be conducted but could potentially be due to immigration or influences of the tidal cycle.

Consumption of Mysids

Although many Chesapeake Bay fishes are thought to consume mysids, we found relatively few predators constituted most of the mysid predation. We selected fish species for examination based on a pilot study in 2022 and scientific literature. Mysids had made up 5.5% of the Atlantic croaker stomach contents wet weight and 8.3% of the white perch stomach contents wet weight based on various surveys during 2002–2012 in Chesapeake Bay (Idhe et al., 2015). White perch and silver perch accounted for the largest proportions of mortality, and both species are likely to consume mysids as they transition through ontogenetic stages (Waggy et al., 2007,

Clermont & Overton 2015, Pfirrmann & Seitz 2019). Silver perch in the Gulf of Mexico consume mysids when they are larger than 15 mm, and white perch 80-90 mm in the Albermarle sound of North Carolina have exhibited predation on mysids (Waggy et al., 2007, Clermont & Overton 2015). White perch prey upon small invertebrates, including mysids, increasingly as they develop throughout their juvenile stages, but mysids were >20% of the stomach contents in Albemarle Sound (Clermont & Overton 2015). Members of the Sciaenid family made up most of the other potential mysid predators caught in the seine survey, many of which were expected to prey on mysids in their juvenile stages (Sardiña & Lopez 2005, Buchheister & Latour 2015). However, spot, Atlantic croaker, black drum, and spotted sea trout comprised a relatively small portion of our estimated predation mortality. In particular, we observed relatively little predation of mysids by Atlantic croaker, whereas Idhe et al. (2015) reported that mysids had made up 5.5% of the Atlantic croaker stomach contents wet weight in Chesapeake Bay. Our sampling did not take place in waters as deep as those sampled by Buchheister & Latour (2015) and Idhe et al. (2015), which could partially explain differences in the sciaenid consumption of mysids reported. Black drum and spotted sea trout had low estimated abundance that explains their minor contributions to mysid predation mortality. Buchheister & Latour (2015) suggested that different life stages of fish may have quite different diets.

Dissection Findings

Many of the fish species in our study consumed mostly taxa other than mysids. This may be due to differences in preference of fish, or due to the availability of different types of prey. Because we were focusing on predation impacts specifically on mysids, we did not quantify the other prey that make up the prey field, so we cannot confirm if the presence of mysids or other organisms in the stomachs are due to the preference of the fish or availability of the prey. Species

like spot and Atlantic croaker are adapted for bottom feeding and often consume benthic infauna such as polychaetes (Chao & Musick 1977, Hines et al., 1990, Idhe et al., 2015, Willis et al., 2015, Pfirrmann & Seitz 2019), which was also supported by our dissection results. The other species we observed, while morphologically able to consume mysids, may have sought other types of prey, which could explain the paucity of mysids in their stomach contents. Black drum tend to select bivalves in feeding (Mendenhall 2015) and in addition to spotted sea trout, were not frequent in our sampling. Atlantic menhaden filter feed on small zooplankton and phytoplankton (Jeffries 1975, Lewis & Peters 1994), and halfbeak are expected to consume seagrasses and microalgae (Collette 1999). Atlantic needlefish tend to be piscivorous (Bortone 1987, A3), so relatively few mysids in their stomachs is consistent with other studies.

Preliminary Study

Our estimates of mysid consumption and daily mortality rates were substantially higher than from a pilot study we conducted in 2022. In the pilot study, we used similar methods to quantify fish consumption on mysid populations as this study. However, seine collections of fish were mostly during the daytime, which captured a less diverse portion of the fish community with little evidence of predation on mysids. Only spot and spotted sea trout were found to have consumed mysids, which resulted in relatively low predation mortality rate estimates ($<0.05\% d^{-1}$). The pilot study also included one nighttime sampling event, and white perch and Atlantic needlefish were caught and had substantial numbers of mysids in their stomachs. In particular, white perch had consumed substantially more mysids than the spot from the day seines. Because of this difference in predation estimates, we used night seining for fish sampling in 2023. The differences in mysid consumption estimates were most likely due to changes in the assemblage of fish in our study area between day and night. It is unlikely that the fish are consuming more or

fewer mysids than they would in the daytime as the presence of mysids in the stomach contents of spot and Atlantic needlefish were similar in both studies. It is also unlikely that the differences were due to diel effects on evacuation of mysids from the fish stomachs, because spot predation mortality of mysids was similar in both studies ($0.003\% \text{ d}^{-1}$ in 2022 and $0.001\% \text{ d}^{-1}$ in 2023).

General Assumptions

Our analyses included a number of important assumptions. First, we assumed that the mysids and fish were randomly distributed in our study area. Mysids had higher density at the pier sampling site compared to the open water or deeper water sites. Within the study area are several other docks, pilings, and oyster aquaculture cages, and the combination of epibenthic sled tows in structured and open habitats likely captures real variability of mysid abundance in the area. While many fish tend to follow their prey, from deeper waters (Methven et al 2001, Ludsin et al 2009) to more shallow waters at night, sampling exclusively in the shallower regions of our study may underestimate the fish abundances in our study area. For many of the fish species we caught, underestimates would not have a significant effect on the predation mortality, as most of the predation was a result of silver perch and white perch. If we underestimated the abundances of these two species, the overall predation on these nearshore mysids would be underestimated as well. We also assumed that the epibenthic sled has a catchability of 100% for mysids. Because of this assumption, the estimates of mysid abundance are likely conservative. Allen (1984) suggests that epibenthic sled sampling probably underestimates mysid abundance. If mysid abundance is higher than we estimated, predation mortality on mysids would in turn be lower than we estimated. We assumed that the abundance of each fish species was independent of the others and independent of mysid abundances. This assumption of independence appears warranted because the correlations of abundance among fish species and mysids were not significant (Table

A1.2). We also assumed that the fish species observed in our survey were the only ones present in the study area. However, literature suggests that other fish such as summer flounder and striped bass are common predators of mysids but were not caught in our seines despite historically being found in the area (Boynton et al., 1981, Wingate & Secor 2008, Buchheister & Latour 2011, Idhe et al., 2015). Thus, there is potential that our estimates of predation were underestimated.

Conclusion

Predation on *Americamysis* spp. by nearshore finfish species near the mouth of the Patuxent River, Maryland appeared to be an important source of mortality. The rates of predation mortality we estimated were similar to estimates from other mysid species, but there were large differences in estimates in literature. These differences may be due to the smaller sampling size, the difference in study location, the drivers of mortality in the different studies (predation, age, diet, etc.), the type of study (experimental versus *in situ*), or estimation method. Using *in situ* data, such as those presented in this paper, was important to not only document the predators that may be affecting *Americamysis* spp. populations, but to accurately model the Chesapeake Bay food web.

Tables*Table 1.1: Dates of the mysid survey and seine survey.*

Epibenthic Sled Dates	Seine Dates
08/17/2023	08/15/2023
08/24/2023	08/31/2023
08/31/2023	09/15/2023
09/07/2023	09/18/2023
09/15/2023	09/18/2023
09/28/2023	

Table 1.2: Species of fish caught in the seine survey, the number of each species (Num Spp.), the length ranges for each species, and the mean length of each species. Abbreviations for the fish species are Atlantic croaker (AC), Atlantic needlefish (AN), black drum (BD), halfbeak (HB), Atlantic menhaden (AM), silver perch (SP), southern kingfish (SK), spot (ST), spotted sea trout (SS), weakfish (WF), white perch (WP).

Species	Num Spp.	Length Range (mm)	Mean Length (mm)
AC	12	115–212	162.9
AN	81	216–565	311.3
BD	1	144	144
HB	11	141–226	167.5
AM	3	82–102	95
SP	10	72–127	99.7
SK	2	150–151	150.5
ST	8	87–163	111.8
SS	1	174	174
WF	1	107	107
WP	5	92–103	190.6

Table 1.3: Summary of stomach contents data of finfish from beach seine sampling in the lower Patuxent River during August-September, 2023. Species of fish (Spp. Fish) that were dissected are listed in the first column, followed by the total number of fish examined (Tot. Fish) and the total number of mysids consumed (Tot Mys.). The proportion (Prop.) of individuals in each species of fish found to have the identified prey item are provided by prey taxa: amphipods (Amp.), fish, insects (Ins.), polychetes (Poly), crabs, foliage (Fol.), shrimp (Shr.), and isopods (Isop.). See Table 1.2 for fish species name abbreviations.

Spp. Fish	Tot. Fish	Tot. Mys.	Prop. Mys.	Prop. Amp.	Prop. Fish.	Prop. Ins.	Prop. Poly.	Prop. Crabs	Prop. Fol.	Prop. Shr.	Prop. Isop.
AC	12	13	0.25	0.50	0.17	0.00	0.42	0.17	0.00	0.00	0.17
AN	81	1	0.012	0.012	0.46	0.05	0.72	0.00	0.00	0.00	0.01
BD	1	0	0.00	0.00	0.00	0.00	1.0	0.00	0.00	0.00	0.00
HB	11	0	0.00	0.00	0.00	0.00	0.55	0.00	0.27	0.00	0.00
AM	3	0	0.00	0.00	0.00	0.00	0.00	0.00	0.00	0.00	0.00
SP	10	163	0.90	0.30	0.20	0.00	0.30	0.00	0.00	0.10	0.00
SK	2	28	1.0	0.50	0.00	0.00	0.00	0.00	0.00	0.50	0.00
ST	8	1	0.13	0.25	0.0	0.00	0.38	0.00	0.00	0.00	0.00
SS	1	0	0.00	0.00	1.0	0.00	0.00	0.00	0.00	0.0	0.00
WF	1	60	1.0	0.00	0.00	0.00	0.00	0.00	0.00	0.00	0.00
WP	5	424	0.80	0.20	0.40	0.00	0.20	0.00	0.00	0.00	0.00

Figures

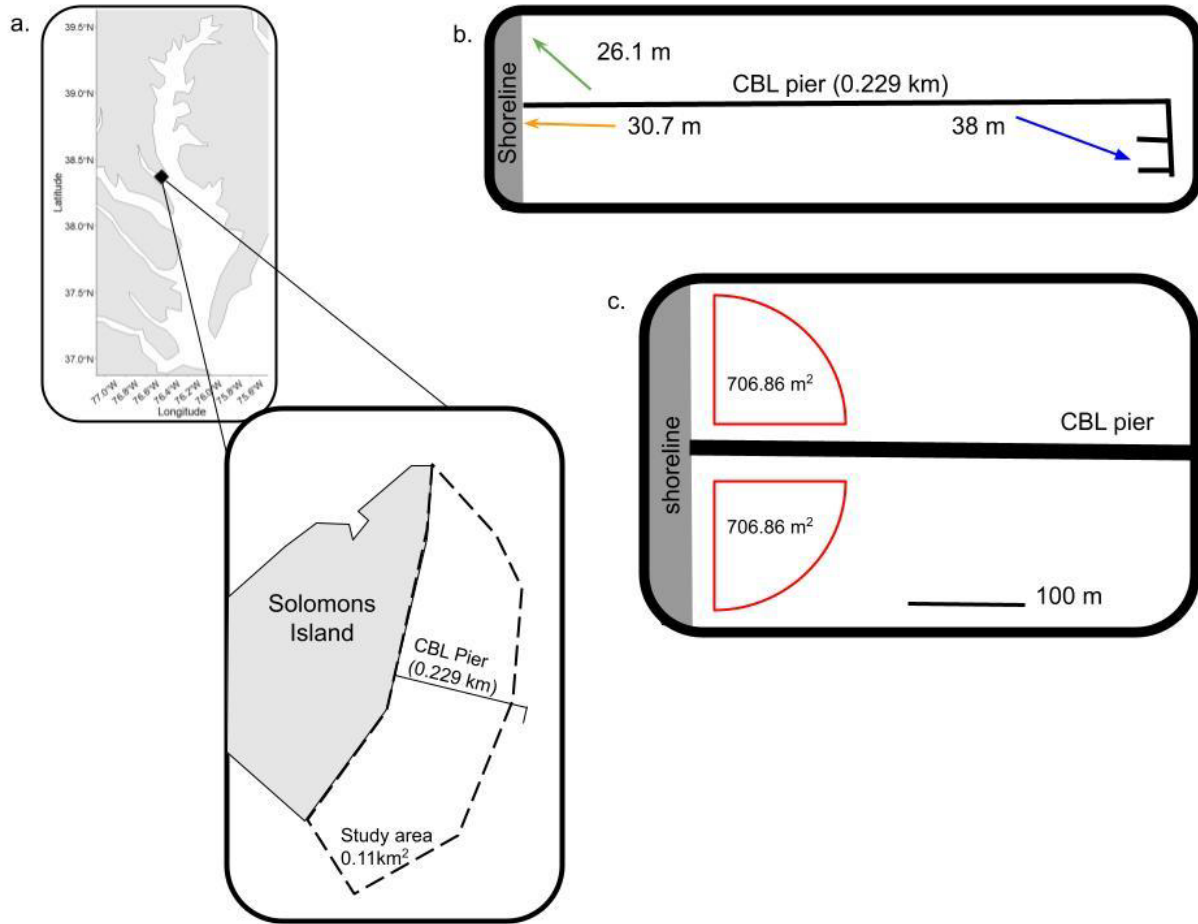


Figure 1.1: Study location in the lower Patuxent River, Maryland, U.S.A. with the study area represented by a dashed line (a), an aerial view of the Chesapeake Biological Laboratory (CBL) Research Pier with arrows indicating the locations and directions of epibenthic sled tows (b), and a zoomed in aerial view of the CBL Research Pier with seine sampling areas in red. The orange arrow represents the structured tow parallel to the pier (Pier). The green arrow represents the shallow open water tow (Open). The blue arrow represents the deep water tow (Deep).

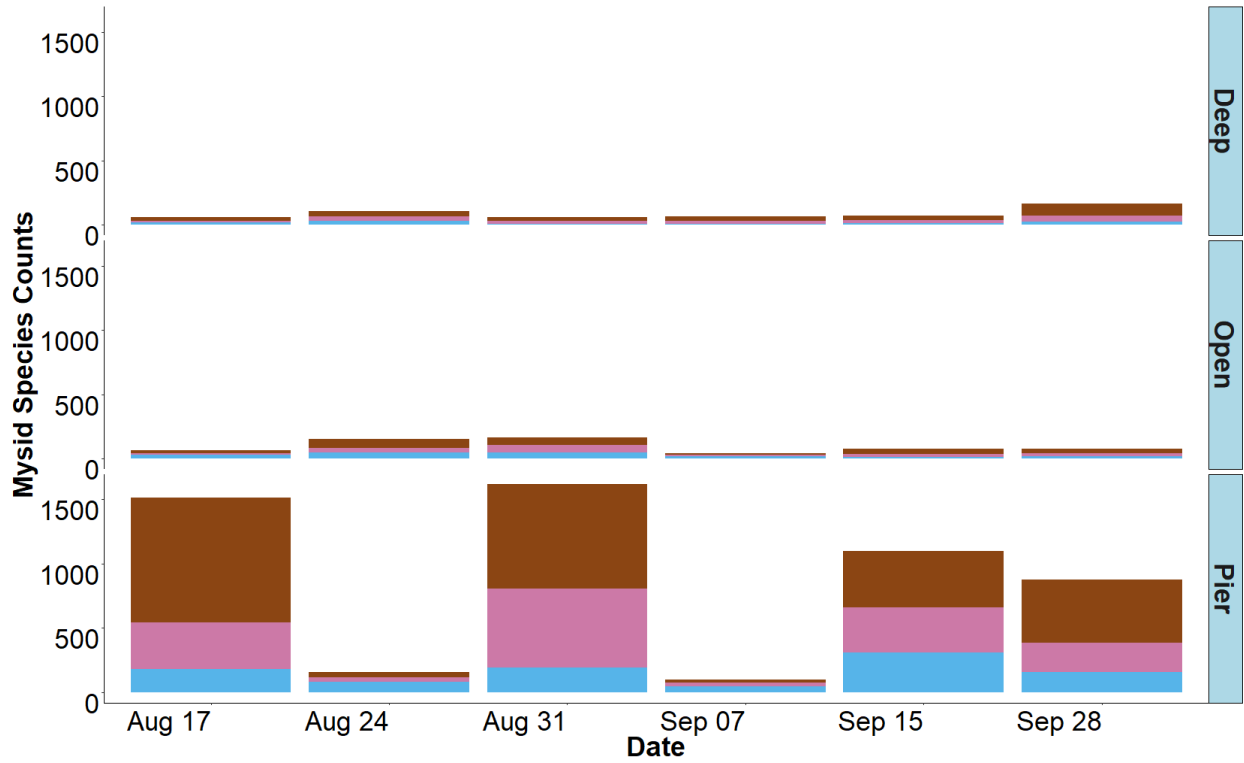


Figure 1.2: Counts of mysids from each epibenthic sled tow (rows) for each mysid sampling day (columns). Transects are described in Figure 1.1b. Catches of each species are represented by colors: *Americamysis almyra* in brown, *A. bahia* in pink, and *A. bigelowi* in light blue.

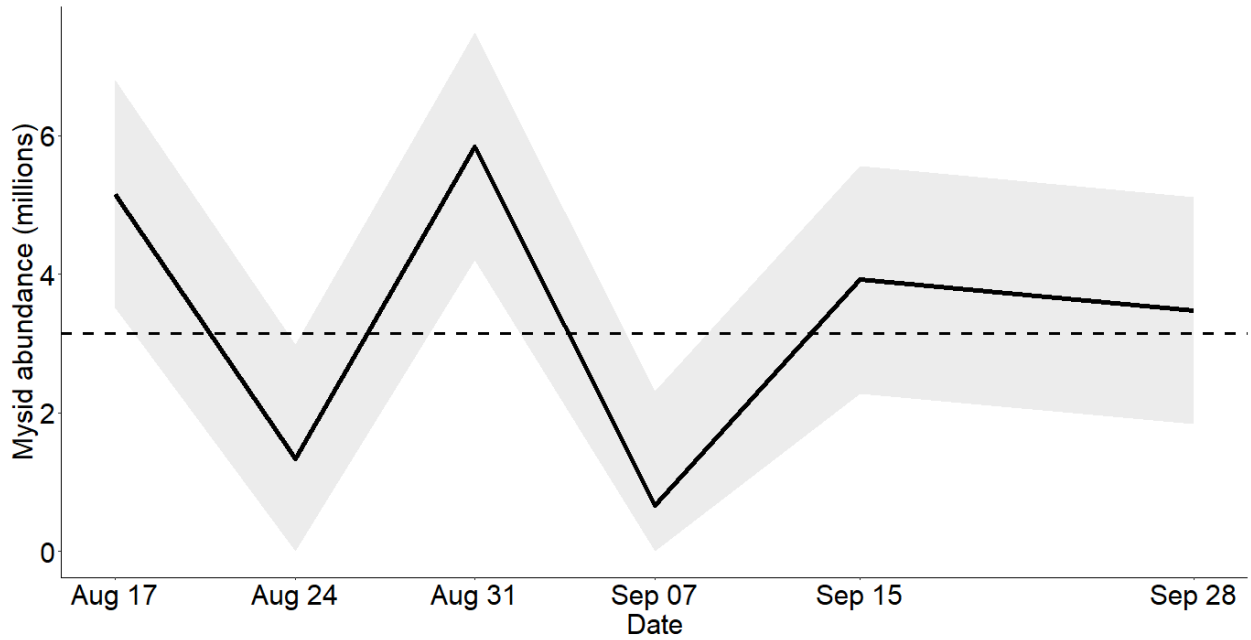


Figure 1.3: Estimated daily abundance of mysids (solid line), 95% confidence intervals (shaded area), and mean mysid abundance (dashed line) in the lower Patuxent River sampling area. Abundance estimates were calculated using non-parametric bootstrapping.

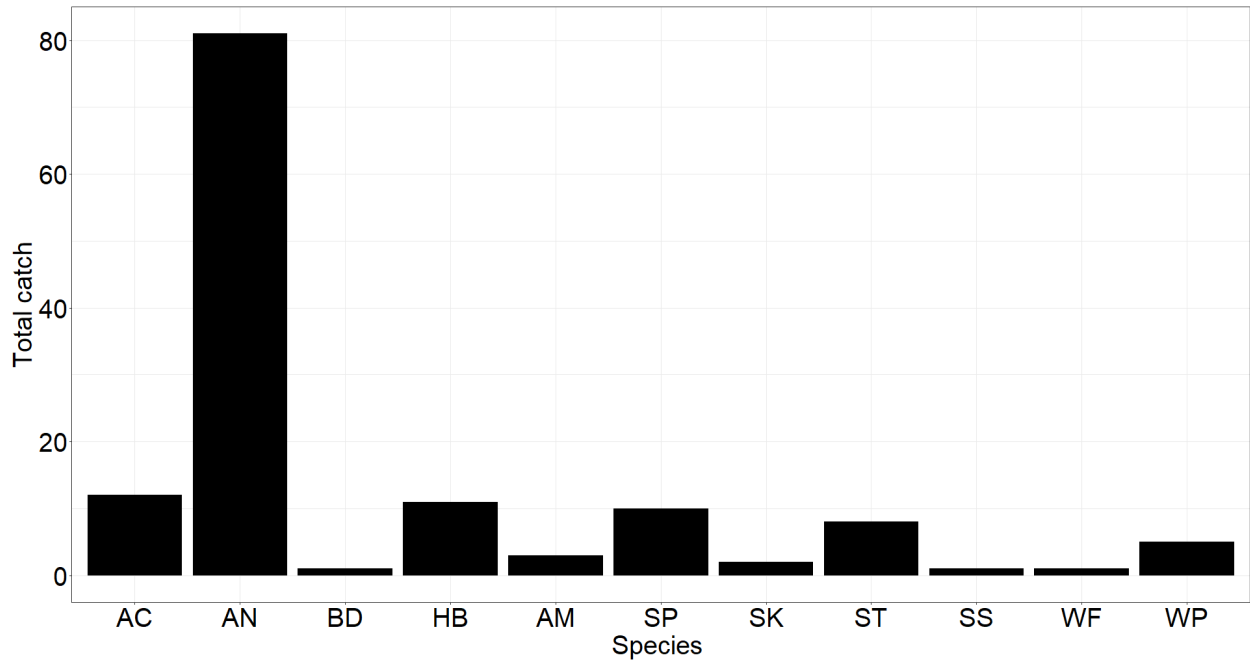


Figure 1.4: Number of fish caught by species in beach seine sampling in the lower Patuxent River during August–September, 2023. See Table 1.2 for fish species name abbreviations.

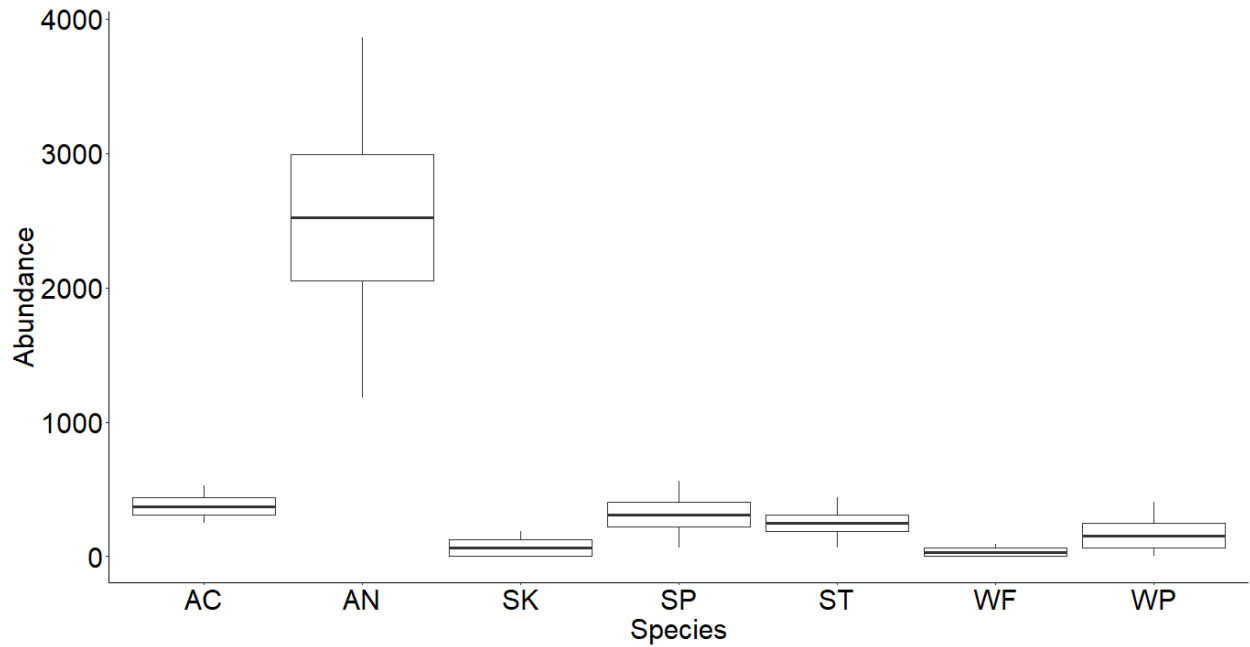


Figure 1.5: Estimated abundance of fish species that consumed mysids from beach seine samples in the lower Patuxent River during August–September, 2023. The box plots represent results from 10,000 non-parametric bootstrap replicates. The heavy lines indicate the median of the abundance estimates for each species, the boxes indicate the 25th and 75th percentiles, and the whiskers represent 95% confidence intervals. See Table 1.2 for species name abbreviations.

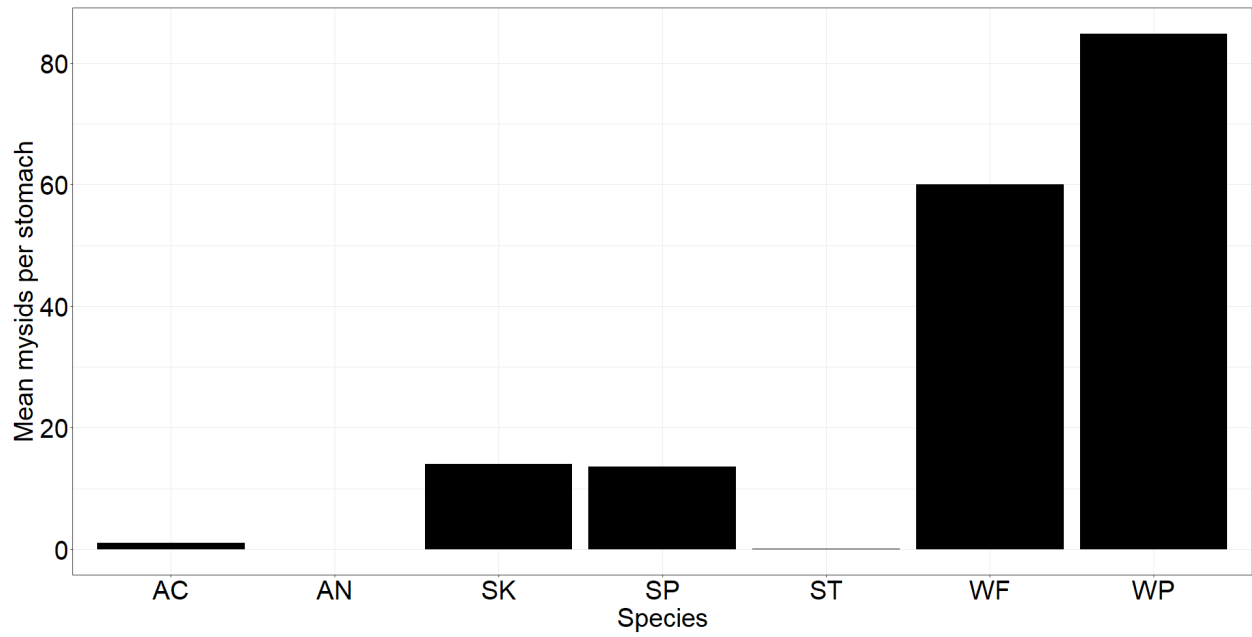


Figure 1.6: The mean number of mysids per stomach by fish species from the lower Patuxent River during August-September, 2023. The value of mean mysids per stomach for Atlantic needlefish was $0.012 d^{-1}$ and $0.053 d^{-1}$ for spot. See Table 1.2 for species name abbreviations.

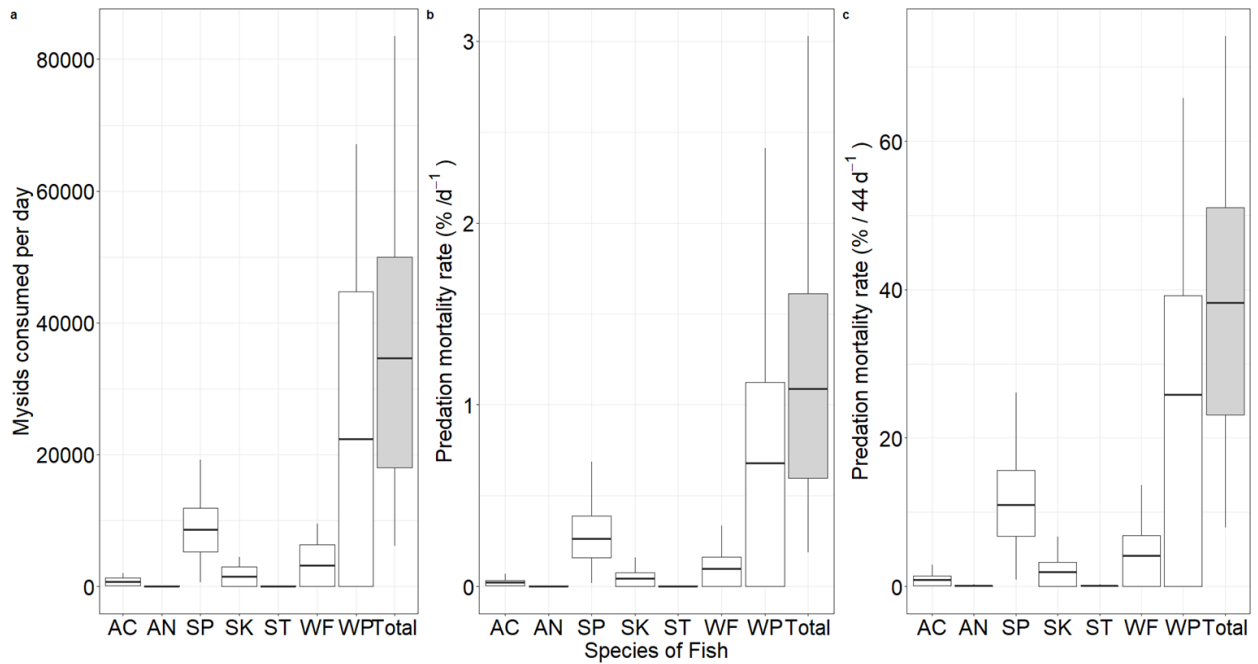


Figure 1.7: Estimated daily consumption of mysids (a), daily predation mortality rates (b), and 44-day predation mortality rates (c) by fish species and all species combined (Total) in the lower Patuxent River during August–September, 2023. The definitions of the boxes and whiskers are the same as those in Figure 1.5. See Table 1.2 for species name abbreviations.

References

- Boscarino, B. T., Oyagi, S., Stapylton, E. K., McKeon, K. E., Michels, N. O., Cushman, S. F., & Brown, M. E. (2020). The influence of light, substrate, and fish on the habitat preferences of the invasive bloody red shrimp, *Hemimysis anomala*. *Journal of Great Lakes Research*, *46*, 311–322. <https://doi.org/10.1016/j.jglr.2020.01.004>
- Boynton, W. R., Zion, H. H., & Polgar, T. T. (1981). Importance of Juvenile Striped Bass Food Habits in the Potomac Estuary. *Transactions of the American Fisheries Society (1900)*, *110*, 56–63. [https://doi.org/10.1577/1548-8659\(1981\)110<56:IOJSBF>2.0.CO;2](https://doi.org/10.1577/1548-8659(1981)110<56:IOJSBF>2.0.CO;2)
- Buchheister, A., & Latour, R. J. (2011). Trophic Ecology of Summer Flounder in Lower Chesapeake Bay Inferred from Stomach Content and Stable Isotope Analyses. *Transactions of the American Fisheries Society (1900)*, *140*, 1240–1254. <https://doi.org/10.1080/00028487.2011.618364>
- Buchheister, A., & Latour, R. J. (2015). Diets and trophic-guild structure of a diverse fish assemblage in Chesapeake Bay, U.S.A. *Journal of Fish Biology*, *86*, 967–992. <https://doi.org/10.1111/jfb.12621>
- Chao, L. N., & Musick, J. A. (1977). Life history, feeding habits, and functional morphology of juvenile sciaenid fishes in the York River Estuary, Virginia. *Fish. Bull.* *75*, 657-702.
- Clermont, J. J., & Overton, A. S. (2015). Tracking ontogenetic food habits of early life stages of white and Yellow perch in Albemarle Sound, North Carolina. *Journal Of The North Carolina Academy of Science*, *131*, 2–12. <https://Doi.Org/10.7572/2167-5872-131.1.2>
- Clutter, R.I., Thielacker, G. (1971). Ecological efficiency of a pelagic mysid shrimp. Estimates from growth, energy budget, and mortality studies. *Fish. Bull. U.S.*, *69*, 93–115.

- Collette, B.B. (1999). Hemiramphidae. halfbeaks. p. 2180-2196. In K.E. Carpenter and V. Niem (eds.) *FAO species identification guide for fishery purposes*. The living marine resources of the Western Central Pacific. Vol. 4. Bony fishes part 2 (Mugilidae to Carangidae). FAO, Rome.
- Connell, A. D. (2008). New species of mysids (Crustacea: Mysidae) from the east coast of South Africa, with notes on habitat preferences. *African Natural History*, 4, 1–10.
- Efron, B., and R.J. Tibshirani. 1994. An Introduction to the Bootstrap. Monographs on Statistics and Applied Probability 57. Chapman and Hall/CRC Press. New York
<https://doi.org/10.1201/9780429246593>
- Eggers D.M. (1977). Factors in interpreting data obtained by diel sampling of fish stomachs. *J. Fish. Res. Board Can.*, 34, 290–294.
- Gergs, R., Hanselmann, A. J., Eisele, I., & Rothhaupt, K.-O. (2008). Autecology of *Limnomysis benedeni* Czerniavsky, 1882 (Crustacea: Mysida) in Lake Constance, Southwestern Germany. *Limnologica*, 38, 139–146. <https://doi.org/10.1016/j.limno.2007.12.002>
- Guedes, É. H. L., Pereira, J. A., Brito, G. J. S., Júnior, A. da G. F. V., & Pessanha, A. L. M. (2024). Predation Risk, Foraging and Reproduction of an Insectivore Fish Species Associated with Two Estuarine Habitats. *Diversity (Basel)*, 16, 707.
<https://doi.org/10.3390/d16110707>
- Hines, A. H., Haddon, A. M., & Wiechert, L. A. (1990). Guild structure and foraging impact of blue crabs and epibenthic fish in a subestuary of Chesapeake Bay. *Marine Ecology Progress Series*, 67, 105–126. <https://doi.org/10.3354/meps067105>

- Ihde, T.F., E.D. Houde, C.F. Bonzek, and E. Franke. (2015). Assessing the Chesapeake Bay Forage Base: Existing Data and Research Priorities. STAC Publication Number 15-005, Edgewater, MD. 198 pp.
- Ikeda, T. (1992). Growth and life history of the mesopelagic mysid *Meterythrops microphthalmus* in the southern Japan Sea. *J. Plankton Res*, 14, 1767–1779.
<https://doi.org/10.1093/plankt/14.12.1767>
- Jeffries, H. P. (1975). Diets of juvenile Atlantic menhaden (*Brevoortia tyrannus*) in three estuarine habitats as determined from fatty acid composition of gut contents. *Canadian Journal of Fisheries and Aquatic Sciences*, 32, 587–592. <https://doi.org/10.1139/f75-075>
- Kuhn, A., Munns Jr, W. R., Poucher, S., Champlin, D., & Lussier, S. (2000). Prediction of population-level response from mysid toxicity test data using population modeling techniques. *Environmental Toxicology and Chemistry*, 19(9), 2364–2371.
<https://doi.org/10.1002/etc.5620190929>
- Lewis, V. P., & Peters, D. S. (1994). Diet of Juvenile and Adult Atlantic Menhaden in Estuarine and Coastal Habitats. *Transactions of the American Fisheries Society (1900)*, 123, 803–810. [https://doi.org/10.1577/1548-8659\(1994\)123<0803:DOJAAA>2.3.CO;2](https://doi.org/10.1577/1548-8659(1994)123<0803:DOJAAA>2.3.CO;2)
- Ludsin, S. A., Zhang, X., Brandt, S. B., Roman, M. R., Boicourt, W. C., Mason, D. M., & Costantini, M. (2009). Hypoxia-avoidance by planktivorous fish in Chesapeake Bay: Implications for food web interactions and fish recruitment. *Journal of Experimental Marine Biology and Ecology*, 381, S121–S131.
<https://doi.org/10.1016/j.jembe.2009.07.016>

- Mayor, E., Chigbu, P., Pierson, J., & Kennedy, V. S. (2017). Composition, abundance, and life history of mysids (crustacea: Mysida) in the coastal lagoons of MD, USA. *Estuaries and Coasts*, 40, 224–234. <https://doi.org/10.1007/s12237-016-0131-z>
- Mayor, E. D., & Chigbu, P. (2018). Mysid shrimp dynamics in relation to abiotic and biotic factors in the coastal lagoons of Maryland, Mid-West Atlantic, USA. *Marine Biology Research*, 14, 621–636. <https://doi.org/10.1080/17451000.2018.1472384>
- McGrath, P., & Austin, H. A. (2009). Site Fidelity, Home Range, and Tidal Movements of white Perch during the Summer in Two Small Tributaries of the York River, Virginia. *Transactions of the American Fisheries Society*, 138, 966–974. <https://doi.org/10.1577/T08-176.1>
- Mees, J., Abdulkerim, Z., & Hamerlynck, O. (1994). Life history, growth and production of *Neomysis integer* in the Westerschelde estuary (SW Netherlands). *Marine Ecology Progress Series*, 109, 43–57. <https://doi.org/10.3354/meps109043>
- Mendenhall, K. S. (2015). *Diet of black drum (Pogonias cromis) based on stable isotope and stomach content analyses*. [Master's Thesis], Texas A&M University Corpus Christi].72pp. <http://hdl.handle.net/1969.6/660>
- Methven, D.A, R.L Haedrich, and G.A Rose. (2001) The fish assemblage of a Newfoundland estuary: diel, monthly and annual variation. *Estuarine, Coastal and Shelf Science* 52: 669–687. <https://10.1006/ecss.2001.0768>
- Pfaffmann, B. W., & Seitz, R. D. (2019). Ecosystem services of restored oyster reefs in a Chesapeake Bay tributary: abundance and foraging of estuarine fishes. *Marine Ecology Progress Series*, 628 155–169. <https://doi.org/10.3354/meps13097>

- Quill, D. M. (2024). *Spatiotemporal Distribution of Chesapeake Bay Mysids in the Choptank and Patuxent Rivers, Maryland*. [Master's Thesis]. University of Maryland Center for Environmental Science. 82pp. <https://doi.org/10.13016/eep1-c7hr>
- Sardiña, P., & Lopez Cazorla, A. C. (2005). Feeding habits of the juvenile striped weakfish, *Cynoscion guatucupa* Cuvier 1830, in Bahía Blanca estuary (Argentina): seasonal and ontogenetic changes. *Hydrobiologia*, 532, 23–38. <https://doi.org/10.1007/s10750-004-8769-0>
- Waggy, G. L., Peterson, M. S., & Comyns, B. H. (2007). Feeding habits and mouth morphology of young silver perch (*Bairdiella chrysoura*) from the north-central Gulf of Mexico. *Southeastern Naturalist*, 6, 743–751. [https://doi.org/10.1656/1528-7092\(2007\)6\[743:FHAMMO\]2.0.CO;2](https://doi.org/10.1656/1528-7092(2007)6[743:FHAMMO]2.0.CO;2)
- Willis, C. M., Richardson, J., Smart, T., Cowan, J., & Biondo, P. (2015). Diet composition, feeding strategy, and diet overlap of 3 sciaenids along the southeastern United States. *Fishery Bulletin*, 113, 290–301. <https://doi.org/10.7755/FB.113.3.5>
- Wingate, R. L., & Secor, D. H. (2008). Effects of winter temperature and flow on a summer-fall nursery fish assemblage in the Chesapeake Bay, Maryland. *Transactions of the American Fisheries Society*, 137, 1147–1156. <https://doi.org/10.1577/t07-098.1>

Chapter 2: Using DNA metabarcoding to characterize mysid diets in the Chesapeake Bay

Introduction

Mysid Overview

Mysids are abundant supra-benthic organisms in many marine, estuarine, and freshwater ecosystems (Dean et al., 2005, Rappé et al., 2011, Mayor et al., 2017, Omweri et al., 2021, Oliveira et al., 2023). They connect benthic and pelagic habitats by transporting energy and nutrients throughout the water column (Fockedey & Mees 1999, Dean et al., 2005, Mayor et al., 2018, Griffin et al., 2020, Kiljunen et al., 2020, Omweri et al., 2021, Oliveira et al., 2023). Their size and high abundance also make them important prey for fish and crustaceans (Dean et al., 2005, Rappé et al., 2011, Oliveira et al., 2023). Although mysids can affect the availability of their prey, (Laprise & Dodson 1994, Wilhelm et al., 2002) and are prey for fish and invertebrates in many aquatic food webs (Oliveira et al., 2023), relatively little is known about *in situ* feeding of mysids.

Mysids in Food Webs

Mysids are typically described as trophic generalists and can rely on various types of prey depending on the time of year, benthic or pelagic association, local prey composition, and their size (Mauchline 1980, Fockedey & Mees 1999, Johannsson et al., 2001, Winkler et al., 2007, Hrycik et al., 2015, Nakamura et al., 2020, Oliveira et al., 2023). Mysids have been described as herbivorous, detritivorous, carnivorous, or omnivorous depending mainly on species, sampling season and ontogenetic stage (Fockedey & Mees 1999, Lehtiniemi et al., 2002, Nakamura et al., 2020, Oliveira et al., 2023). Diets of mysids often consist of diatoms, dinoflagellates, and other phytoplankton (Bowers & Grossnickle 1978, Johannsson et al., 2001, Evans et al., 2018).

Detritus and zooplankton such as copepods and cladocerans contribute more to diets when they are abundant and usually in larger mysids (Johnston & Lasenby 1982, Johannsson et al., 2001, Caldwell et al., 2016, Evans et al., 2018). Hanselmann et al., (2013) found that mysids prefer prey items like phytoplankton and detritus over animal prey as exhibited by *Limnomysis benedeni* stomach contents. Wilhelm et al., (2002) suggested a preference for *Daphnia* by *Tenagomysis chiltoni* even when amphipods were available. There is also evidence that mysids consume vascular plants although some species may exhibit a preference for phytoplankton over vascular plant materials *in situ* (Zagursky & Feller 1985, Fockedy & Mees 1999, Chew et al., 2012).

Mysid Feeding Modes

There are a range of different modes of feeding that mysids use (Viitasalo & Rautio 1998, Lehtiniemi et al., 2002, Kouassi et al., 2006). Many studies support that mysids typically create currents with the exopods on their thorax to bring potential food items towards their mouths (Mauchline 1980, Siegfried & Kopache 1980, Fockedy & Mees 1999, Borza et al., 2023). This current-production method works well for most microalgae and detritus, and some smaller zooplankton. However, mysids may also switch to a raptorial feeding method depending on types of prey present, often in the presence of larger zooplankton (Mauchline 1980, Viitasalo & Rautio 1998, Lehtiniemi et al., 2002).

Diet Methodology

Multiple methods are used for analyzing diets of organisms *in situ*, some of which have already been applied to understand mysid diets. The most common approaches include visual identification of stomach contents and stable isotope analysis of mysids and prey, both of which

have limitations. When visual identification is used to study the stomach contents of small organisms like mysids, it can often be difficult to correctly identify items or remnants of items due to their already small sizes and degradation during ingestion and digestion (Wilhelm et al., 2002, Gorokhova 2009, Evans et al., 2018, Yeh et al., 2020, Holmes & Kimmerer 2022, Chae et al., 2023). Use of stable isotopes can explain the trophic level of an organism, the general trophic levels of their prey, and the dominant trophic pathways contributing to the diet, but it often lacks specificity regarding individual prey taxa and typically requires sufficient concurrent stable isotope analysis of prey or basal trophic resources to properly interpret the results (Johannsson et al., 2001, Lesutienė et al., 2008, Evans et al., 2018, Nakamura et al., 2020).

DNA metabarcoding is a modern high-throughput molecular identification method that is increasingly used in ecological studies (Taberlet et al., 2012). It assigns taxonomic identifications to fragments of DNA that have been extracted and amplified from environmental or biological samples (Taberlet et al., 2012). DNA metabarcoding can be a useful method in understanding specific taxa in an organism's diet (Gorokhova 2009, Holmes & Kimmerer 2022). Unlike microscopy, no visual identification of the stomach contents is required. DNA metabarcoding also has the potential to identify contents to lower taxonomic levels beyond trophic level and pathway identity (e.g., pelagic, benthic, littoral), where bulk stable isotopes can be limited. Gorokhova (2009) used targeted molecular methods to identify cyanobacteria in the stomachs and fecal pellets of *Mysis mixta* and *Mysis relicta* in an experimental study, and Nakamura et al. (2020) used DNA metabarcoding to identify diet contents of *Neomysis awatschensis* in a freshwater lake in Japan using mysid fecal pellets. Despite the benefits of using molecular methods for understanding mysid diets, no such study has taken place on any mysids in Chesapeake Bay.

Mysids in Chesapeake Bay

There are two prominent genera of mysids that are represented by four species (*Neomysis americana*, *Americamysis almyra*, *A. bahia*, and *A. bigelowi*) in Chesapeake Bay (Cowles 1930). *Neomysis* dominates the region for most of the year, but the more southerly distributed *Americamysis* spp. are abundant in the late summer and fall (Cowles 1930). Given their similar size and spatial overlap, individuals from each of the genera could potentially fill similar roles when they are present in Chesapeake Bay, in linking the microscopic and macroscopic portions of the food webs. Because mysid *in situ* stomach contents have yet to be studied in Chesapeake Bay, our goal was to molecularly identify contents of mysids diets in a natural settings. Our objectives were to 1) develop methods for using DNA metabarcoding to identify the stomach contents of mysids and 2) characterize the diets of mysids in the St. Marys and Patuxent rivers of Maryland.

Methods

Sampling

We collected mysids for DNA metabarcoding from two tributaries of the Chesapeake Bay: the St. Marys River and the Patuxent River. Two sites were sampled in the St. Marys River (Figure 2.1). One site was open to oyster harvest (Site 1) and the other a designated oyster sanctuary where oyster fishing was not allowed (Site 2). Mysids from the St. Marys River were collected between 10:00 AM and 1:00 PM on April 10, 2024, using an epibenthic sled. The epibenthic sled was 0.38 m wide by 0.16 m high with a mesh size of about 1 mm, towed for 3 minutes at depths ranging from 1–2 m. Once collected, ~100 mysids were subsampled from each site and preserved in 95% ethanol until dissection.

The remainder of the specimens came from two sites in the Patuxent River sampled from 9:00 PM on May 16, 2024, to 3:00 AM on May 17, 2024 (Figure 2.1). One site (Site 2) was seasonally hypoxic (experiencing hypoxia in the summer), and sampled at 9:00 PM on May 16, and at 1:30 AM on May 17. The other (Site 5) does not regularly experience hypoxia, and was sampled at 11:30 PM on May 16, and at 3:00 AM on May 17. Mysids from the Patuxent River were collected using a zooplankton net with a 50-cm diameter and 500- μ m mesh towed for 3 minutes. The zooplankton net was deployed twice per station, once to sample at the surface (0.25 m deep) of the water column and again to sample the middle of the water column in waters 3–6 m deep. Once collected, ~100 mysids were subsampled from each site and preserved in 95% ethanol until dissection.

Sampling in the St. Marys and Patuxent rivers was conducted separately because we were attempting to answer different questions about mysid diets in each river, and we were unable to sample both rivers within a similar time frame. There was no intent to compare the two rivers in one analysis.

Dissections

An initial study was conducted to determine the amount of genetic material necessary for DNA metabarcoding. Samples of 1–4 mysid stomachs (three replicates of each) were sent to the Smithsonian Environmental Research Center (SERC) for initial analysis. Genomic DNA was extracted using a Qiagen Blood and Tissue kit following the manufacturer's protocol with an overnight digestion in proteinase K. Concentration of genomic DNA was calculated using a NanoDrop spectrophotometer. Only the vials containing four stomachs had sufficient concentrations of DNA for polymerase chain reaction (PCR; 21.7–36.1 [DNA] ng/ μ L, and

260/280 wavelength ratios between 2.51–3.00). Therefore, we combined four mysid stomachs per sample from each site and time for all subsequent analyses.

Mysid stomachs were removed using forceps and a dissection needle. Flame-ethanol sterilization was used in between each individual mysid dissection to prevent cross contamination of samples. Mysids were dissected using an Olympus SZX16 dissecting microscope at $1 \times$ PF objective magnification and an ocular magnification of 0 with a $3.2 \times$ zoom ratio. For each dissection, the mysid was speciated and measured to the nearest hundredths of a millimeter with a $7 \times$ zoom ratio using the ImageJ-win64 software. Next, the mysids were rinsed of ethanol with DI water, and the stomach was removed by holding back the carapace with the forceps and removing the organ from the rest of the abdomen with the dissection needle. The stomach was then placed into a 1.5-ml DNase/RNase-free tube. Each tube contained four stomachs of mysids from the same location and sampling time, representing one sample in our study. After the dissections for each sample tube were completed, the sample was frozen at -50°C until the metabarcoding took place. For St. Marys River, we had five samples from each site on the river, for a total of 10 St. Marys samples. From the Patuxent we had 20 samples from each site and time combination (21 from the earliest station visit, as there was one extra sample space available), for a total of 81 samples. Therefore, a total of 91 samples of mysid stomach contents were analyzed using metabarcoding.

DNA Metabarcoding and Bioinformatics

DNA was extracted using the Qiagen DNEasy Blood and Tissue spin column kit protocols for animal tissue for all steps except for elution. We used proteinase K to digest each sample overnight to extract the DNA. We extracted the entirety of each sample, due to the small

volume of mysid stomachs, and then eluted to 40 μL (half of the standard elution volume) to increase the concentration of DNA.

The primers 3NDeukF and V4eukR1R2 (Bråte et al., 2010) were used to amplify and sequence an approximately 5-600 basepair fragment of the 18S gene, as it is highly conservative for eukaryotes covering a wide range of what mysids are likely to eat (Hagenbüchle et al., 1978). The PCR called for 3 μL of DNA template, 12.28 μL of DNase/RNase free water, 0.8 μL Bovine Serum Albumin, 2 μL PCR buffer, 1.2 μL MgCl_2 , 0.4 μL nucleotides, 0.1 μL forward primer, 0.1 μL reverse primer, and 0.12 μL Taq per sample. Thermocycling steps began with denaturation at 95 $^{\circ}\text{C}$ for 10 minutes, 30 cycles of denaturation at 95 $^{\circ}\text{C}$ for 30 seconds, annealing at 53.2 $^{\circ}\text{C}$ for 45 seconds, and extension at 72 $^{\circ}\text{C}$ for 45 seconds, with a final extension at 72 $^{\circ}\text{C}$ for 5 minutes. Each of the 96 samples underwent PCR in triplicate, and the triplicates were consolidated via pooling based on the intensity of gel electrophoresis bands.

Nextera adapters were used for dual indexing to apply a unique combination for each pooled sample to have bioinformatic separation of the samples. Thermocycling for indexing included a mix of 2 μL of pooled template, 4.5 μL DNase/RNase free water, 6.25 μL KAPA ReadyMix kit, and 1.5 μL of the i5 and i7 primers. The samples were indexed for an initial denaturation at 95 $^{\circ}\text{C}$ for 5 minutes, followed by 12 cycles of denaturation at 98 $^{\circ}\text{C}$ for 20 seconds, annealing at 60 $^{\circ}\text{C}$ for 45 seconds, and extension at 72 $^{\circ}\text{C}$ for 45 seconds, ending with a final extension at 72 $^{\circ}\text{C}$ for 5 minutes. Initially, we used 1 μL of pooled template for 8 cycles rather than 12, which resulted in nearly all of our samples failing to be fully indexed, as the mode of our sequence lengths was 569 basepairs, opposed to an ideal indexed 600 basepair length. Because of this, we increased our number of cycles and volume of pooled template (as described above), which successfully increased the proportion of indexed sequences in our samples (mode

= 592 basepairs). The indexed samples were bead cleaned to remove smaller unwanted fragments and quantified for concentrations following the manufacturer's instructions for the Qubit High Sensitivity double stranded DNA kit. The library was pooled based on equimolar concentrations. Our final library was sequenced using an Illumina MiSeq at the Laboratories of Analytical Biology (Smithsonian National Museum of Natural History).

Analysis

We removed primer sequences using cutadapt (Martin 2011). A software called PHRED was used to assign quality scores to each of the sequences (Richterich 1998). We used the DADA2 package in R to trim sequences based on quality and then removed chimeras and sequences that were too small in length (Callahan et al., 2016). The PR2 database version 5.0.00 was used with the 18S sequences to assign taxonomy to the amplicon sequence variants (ASVs) for identification of individual sequences (Guillou et al., 2013). The default minimum confidence threshold of 50% was used (Callahan et al., 2016).

ASVs were separated into two datasets: one with all mysid sequences excluded, and one with only the consumer-mysid genus sequences excluded (i.e., the genus of the mysid stomach samples). For example, if the mysids in each sample were all *Neomysis*, then only the putative prey sequences that matched with *Americamysis* were kept. This was done to describe a potential proxy for intra-generic cannibalism with the set that included mysids, and to describe the putative prey should this proxy be found unsuitable. Data with the consumer-mysid (mysids that were dissected) sequences were removed. Data that included non-consumer mysid sequences will be referred to as “mysid-included” data, and data from which all mysid sequences were removed will be referred to as “mysid-excluded” data.

The datasets included the sample identification numbers, the river sampled, the date and time sampled, the collection site, mean length of the consumer mysids in each aggregate sample, and water column position for the Patuxent samples (Table A2.1). Samples from the Patuxent River were further categorized into “Night” (09:00 PM and 11:30 PM) and “Morning” (01:30 AM and 3:00 AM). For the ASV-specific data, the assigned family, genus, species, and the abundance (read count) of each ASV were recorded. Additionally, the average length of the adults from each taxon were identified in the sample (average of minimum length and maximum length), and the average size of eggs for those taxa that sexually reproduce were identified using a literature review (referred to as “young of prey”; File S1). For the organisms that do not undergo sexual reproduction (primarily microalgae and protists), the adult sizes were also used for young of prey measurements. For further analysis regarding length of prey, the lengths of young of prey will be used, to separate putative prey that mysids would likely be eating whole. Consumption of organisms larger than the “young of prey” ranges would likely be due to scavenging behaviors, or mechanical breakdown of the prey. Each sequence was also grouped into one of eleven ASV groups: mysids, macroalgae, microalgae (including diatoms, dinoflagellates, and green algae), fungi, protists (excluding those that are diatoms and dinoflagellates), copepods, finfish, tunicates, annelids, hydrozoa, and terrestrial plants. DNA of items in the stomachs may have included parasites in addition to ingested prey. We identified potential parasites among the ASV taxa by determining whether the identified taxa belonged to a genus that included known parasites using a literature review (File S1). We merged sample and DNA metabarcoding datasets for use in further analysis. Genus of prey was used for the length ranges and parasite presence because the 18S gene has not yet yielded high accuracy at species-level identifications in some studies (Dollive et al., 2012, Schoch et al., 2012)

Several analyses were conducted to estimate relationships between ASV or ASV group presence, size, abundance of ASVs (which represent unique detected sequences), and mysid characteristics or sample locations. Analyses were conducted separately for samples from the St. Marys River and the Patuxent River. All analyses and evaluations were done using R (R Core Team 2024). Species richness was examined for all samples from both rivers. We plotted the abundance of each ASV as the dependent variable by sample as the independent variable for the data all together to examine the range in species that were detected. Then, we plotted the abundance (dependent variable) of each unique ASV (independent variable), from the mysid-excluded and mysid-included datasets from each river, to evaluate the relative abundances of each sequence and assess richness within each of the rivers.

We estimated the effect of consumer mysid length on the length of young of prey, to evaluate whether mysids of different sizes were ingesting different sizes of putative prey taxa. If so, differently sized mysids may be affecting different positions of food webs. This was done for all sets of data from both rivers. We used a generalized additive model (GAM) with normally distributed errors, where the dependent variable was length of young of prey (L_{prey}), and the independent variable was the mean sample length of the consumer mysid ($L_{consumer}$),

$$L_{prey} = \beta_0 + s(L_{consumer}) + \epsilon ,$$

where the intercept is represented by β_0 , the s represents the smoothed term, and the error is represented by ϵ .

Because the size of prey may scale with predator size, but the size of parasite likely would not, we ran the same model but with an interaction between length of the consumer mysid and presence of parasites. In this version of the model, a binary variable was included for parasitism ($z_{parasite}$),

$$L_{prey} = \beta_0 + s(L_{consumer}, by = z_{parasite}) + z_{parasite} + \epsilon,$$

where the intercept is represented by β_0 , the $s(L_{consumer}, by = z_{parasite})$ represents the smoothed interaction between consumer mysid length and parasitism, and the error is represented by ϵ . The number of knots in the GAM were set to five for St. Marys River mysid-excluded data because there were too few observations to estimate the number of knots.

GAMs were also used to determine the best predictors of ASV abundance to evaluate the effect of sampling factors on the abundance of ASVs for the St. Marys River. These GAMs used the negative binomial family to account for overdispersion in the abundance data,

$$N_{sequence} = \beta_0 + s(L_{consumer}) + site + \epsilon,$$

where the abundance of sequences was $N_{sequence}$, and the predictor factors were site, and mean length of consumer mysids ($L_{consumer}$), the intercept is β_0 , the s represents the smoothed term, and the error is ϵ . These GAMs all used the negative binomial family to account for overdispersion.

For the Patuxent River samples, water column position (WC) and time of night (t_{night}) were added to the model, and the `mgcv` package automatically selected the number of knots using generalized cross-validation (Wood 2011),

$$N_{sequence} = \beta_0 + s(L_{consumer}) + site + WC + t_{night} + \epsilon,$$

where the intercept is represented by β_0 , the s represents the smoothed term, and the error is represented by ϵ . Similar to the consumer versus putative prey length model, the knots were adjusted only for the St. Marys River mysid-excluded samples. We chose the best model by using Akaike Information Criterion corrected for small sample size (AICc). The best model was determined by the lowest AICc value.

For the Patuxent River mysid-excluded samples specifically, we conducted a GAM to estimate the effect of mysid length, site, time of sampling, and water column position on the presence or absence of non-mysid prey. We did not do this for any of the other data sets, as this was the only dataset in which there were sequences present in the majority of the samples. Presence of prey is designated by z_{prey} , and the binomial family was used due to the binary structure of presence/absence response data. We predicted the effect of each predictor on the presence of prey to determine which variable affected presence of prey the most,

$$z_{prey} = \beta_0 + s(L_{consumer}) + Site + WC + t_{night} + \epsilon,$$

where the intercept is represented by β_0 , the s represents the smoothed term, and the error is represented by ϵ . Similar to the abundance GAMs, we determined the best fit model by ranking AICc values of the individual models.

We evaluated Pearson correlations for binary data (r_P) and co-occurrences of taxa from ASV groups to evaluate the potential for secondary predation or parasitism (i.e., amplification of prey of the prey, or parasites of the prey) (Bowser et al., 2013). We calculated Pearson correlations for binary data between the ASV groups to one another using the *cor* function in R, thus measuring the co-occurrences and joint absences of the ASV groups (R Core Team 2024). We also calculated the proportion (P) of co-occurrences and co-absences of prey group pairs in each sampling group (St. Marys mysid-excluded, St. Marys mysid-included, Patuxent mysid-excluded, Patuxent mysid-included) by calculating the number of samples where both ASV groups were either present ($x_{co-occur}$), or absent ($x_{co-absent}$) divided by the total number of samples (x_{total}),

$$P_{co-occur} = \frac{x_{co-occur}}{x_{total}},$$

$$P_{co-absent} = \frac{x_{co-absent}}{x_{total}}.$$

Results

We collected mysids from both the St. Marys River and the Patuxent River (Figure 2.1). Across all samples, the mean mysid length per sample ranged from 2.49 to 10.32 mm. All of the mysids caught in the St. Marys River were *Americamysis* spp. and had an average mean mysid length of 5.92 mm (ranging 3.70 – 6.84 mm). Most of the mysids caught from the Patuxent River were *Neomysis americana*. Four samples from the Patuxent River were a mixture of *N. americana* and *Americamysis* spp. The average mean mysid length per sample for the Patuxent was 6.46 mm (ranging 2.49 – 10.32 mm).

Post-Sequencing

A total of 12,678,450 sequences were returned from 91 samples and 5 extraction negatives. The number of reads decreased to 6,391,486 sequences after checking for errors, filtering, and denoising; 22,835 (0.36 %) of these sequences were identified as non-mysid taxa. The sequenced data were distributed across 85 ASVs, which are the unique sequences (Table 2.1); 47 of these ASVs were non-mysid taxa. The ASV groups identified from the mysid stomachs included mysids, macroalgae, microalgae (including diatoms, dinoflagellates, and green algae), fungi, protists (excluding those that are diatoms and dinoflagellates), copepods, finfish, tunicates, annelids, hydrozoa, and terrestrial plants (Figure 2.2). The abundances of non-consumer mysid ASVs ranged from 0 to 213,815 individual sequences across samples.

St. Marys River

When mysids were excluded from St. Marys River samples, thirteen unique genera, from sixteen unique ASVs, and six different prey groups were identified. In the mysid-included samples, fourteen unique genera were identified from twenty-two unique ASVs and then grouped into seven ASV groups (Figure 2.3). The ASV groups identified in the samples from the St. Marys River included mysids, microalgae, fungi, protists, copepods, tunicates, and annelids (Table 2.1).

The most abundant non-mysid ASVs in the St. Marys River samples were microalgae, which included diatoms, dinoflagellates, and chlorophytes (Figure 2.3). Microalgae comprised 37.5% (6 of 16) of the ASV sequences by group, excluding mysid taxa. Microalgae made up 5.8% of the total abundance of sequences. The next most common ASV group in numbers of unique ASVs was copepods, which comprised 18.75% of the unique St. Marys ASV counts. Pearson's correlations for binary data of the St. Marys ASV groups were negative between microalgae and tunicates ($r_P = -0.67$, p-value = 0.001, Figure 2.4), and positive between protists and annelids ($r_P = 0.67$, p-value = 0.033). Copepods and fungi also had a relatively strong negative correlation ($r_P = -0.53$, p-value = 0.004). Co-occurrences were rarer than co-absences in St. Marys River, but they were most frequent between mysids and copepods (0.3; Figure 2.4), mysids and fungi (0.4), and mysids and microalgae (0.8). Mysids co-occurred with every other prey group. The ASV groups most likely to both be co-absent were tunicates and annelids (0.8) and annelids and fungi (0.8).

The GAM model of St. Marys putative prey length against mean mysid length was not significant for either the mysid-excluded or mysid-included models (p-value = 0.569, t-value = 0.013; p-value = 0.642, t-value <2e-16; Figure 2.5). Similarly, no relationship was found when

an interaction with parasitism was included in the model (Figure A2.7) for mysid-excluded (parasite absent p-value = 0.667, t-value = 0.016; parasite present p-value = 0.728, t-value = 0.016) or mysid-included samples (parasite absent p-value = 0.625, t-value = $<5e-11$; parasite present p-value = 0.485, t-value = $<5e-11$). Many of the potential parasites (11 of the total unique ASVs) were smaller in size than the other putative prey identified, thus increasing the range of putative prey size across all consumer mysids.

The best predictor of abundance of ASVs was site, where site 1, an oyster reef open to harvesting, had a higher abundance of ASVs than site 2, the oyster sanctuary (p-value = $3.35e-04$; Table A2.2). For mysid-included data, the ASV abundance data were also best explained by site (p-value = $9.51e-05$; Table A2.3).

Patuxent River

In the Patuxent River samples, twenty-four unique genera from 31 unique ASVs and eight different prey groups were identified in mysid-excluded samples. Twenty-five unique genera from 39 unique ASVs were identified and categorized into nine different ASV groups in mysid-included samples. Mysids, macroalgae, microalgae, fungi, protists, copepods, finfish, hydrozoa, and terrestrial plants were the ASV groups identified in sequencing (Table 1, Figure 2.3).

Similar to the St. Marys River samples, the microalgae group had the most ASVs and highest abundance of ASVs after mysids (Figure 2.3). Microalgae made up 38.7% (12 of 31) of the ASV sequences by group and were closely followed by protists which made up 32.3% (10 of 31) of non-mysid ASV groups in the Patuxent River. Microalgae made up 7.1% of abundances of the total Patuxent River non-consumer mysid sequences, and protists made up 3.9%.

Copepods had higher abundance per ASV than protists. Correlations among ASV groups in the

Patuxent River mysid-excluded samples were positive between copepods and protists ($r_p = 0.50$; p -value = 0.046; Figure 2.5), copepods and macroalgae ($r_p = 0.49$; p -value = 0.0256), and copepods and microalgae ($r_p = 0.43$; p -value = 0.043). Co-occurrences were rarer than co-absences in the Patuxent River samples, but mysids co-occurred with all other ASV groups (Figure 2.5). The highest co-occurrence value was 0.12 between mysids and microalgae in the Patuxent. Terrestrial plants, finfish, and hydrozoa only co-occurred with mysids and nothing else.

The results of the GAM for ASV presence in the mysid-excluded Patuxent River samples suggested that only the mean length of the mysids was significantly associated with the presence of ASVs (p -value = $5.54e-05$; Table A2.4; Figure 2.6; Figure 2.7). For mysid-excluded samples, putative prey size was not explained by the length of the consumer mysids (p -value = 0.275, t -value = $3.11e-05$; Figure 2.6). Putative prey size was significantly related to the mean mysid length for the mysid-included samples, in which larger mysids are associated with smaller putative prey (p -value $< 2e-16$, t -value = $< 2e-16$). When an effect for potential parasites was included in the model, the relationship between putative prey size and mysid length was not significant for mysid-excluded data (parasite present p -value = 0.78, t -value = $3.11e-05$; parasite absent p -value = 0.16, t -value = $3.11e-05$; Figure A2.8). There was a significant interaction of parasites on mysid-included data (parasite present p -value = $< 2e-16$, t -value = $< 2e-16$; parasite absent p -value = $1.19e-06$, t -value = $< 2e-16$), indicating that there was a significant difference in consumer mysid length on parasitic prey versus non-parasitic prey. With the introduction of mysids as potential prey, the size range of putative prey expanded for consumer mysids of all sizes.

Mean length of mysids and time of sampling were significantly related to abundance of ASVs in the Patuxent River samples for mysid-excluded data (p-values = $<2e-16$, $5.75e-05$; Table A2.5). Length of mysid, time of sampling, and water column positions had significant effects on abundance of putative prey ASVs for the mysid-included data (p-values = $<2e-16$, 0.005 , $3.18e-07$, respectively; Table A2.6).

Discussion

Mysid Diet Data

We were able to successfully characterize stomach contents of mysids belonging to *N. americana* and *Americamysis* spp. in two Chesapeake Bay tributaries using DNA metabarcoding. A wide range of taxa were identified in the stomachs, but most of the identified ASVs were *N. americana* or *Americamysis* spp. The presence of substantial amounts of mysid DNA was not surprising because we analyzed whole stomachs instead of isolating stomach contents. However, 0.36% (22,835 sequences) of the total sequences belonged to non-mysid taxa, which likely represented predation, secondary predation, or parasitism. This is a lower percentage of non-mysid sequences compared to Nakamura et. al (2020), who used mysids' fecal pellets, and Pagenkopp Lohan et. al (2023) who used striped bass stomachs, larger organisms with larger stomachs. In this study, we eschewed lower levels of taxonomic accuracy for a wider range of identified eukaryotes (Hagenbüchle et al., 1978, Dollive et al., 2012). However, by using PHRED to evaluate the quality of our sequences, and assigning taxon with the PR2 database, the assignments to the genus level are likely accurate (Richterich 1998).

Comparison of Mysid Diets

We found many taxa in the stomach contents that agreed with other studies on mysid diets - primarily diatoms, dinoflagellates, and copepods. Mysids are often described as generalist omnivores, and their prey *in situ* can include diatoms, dinoflagellates, cyanobacteria, other microalgae, ciliates, rotifers, copepods, cladocerans, amphipods, pollen, and detritus (Mauchline 1980, Rudstam et al., 1989, Cartes & Sorbe 1998, Fockedey & Mees 1999, Gorokhova 2009, Takahashi et al., 2015, Caldwell et al., 2016, Evans et al., 2018, Nakamura et al., 2020). Some studies found evidence of other organisms (e.g., polychaetes and cnidarians) that were only occasionally found in mysid stomach contents (Johnston & Lasenby 1982, Rudstam et al., 1989, Cartes & Sorbe 1998). The rarity of these organisms also agrees with the few sequences of polychaetes documented from St. Marys River mysid stomachs in this study. Much of the existing literature on mysid diets comes from freshwater systems, typically lakes. Caldwell et al. (2016) and Johannsson et al. (2001) found that *Mysis diluviana* and *M. relicta* diets changed seasonally, with more zooplankton consumed in the summer months, and more phytoplankton in the spring. We identified substantially higher abundances of microalgae ASVs than zooplankton ASVs, likely due to our springtime sampling. Chesapeake Bay phytoplankton blooms are variable phenomena that take place in the spring and may account for the abundance of microalgae in our mysids' stomachs (Gallegos & Jordan 2002). Nakamura et al. (2020) concluded that while some animal material was present in the fecal pellets of *N. awatschensis* in Lake Kasumigaura, the contents were mostly autotrophic in their June sampling. We observed similar results from our May samples which included some sequences associated with heterotrophs were present, but most belonged to microscopic autotrophs. Hanselmann et al. (2013) found that freshwater *Limnomysis benedeni* preferred microalgae even when animal prey

was present. Other estuarine studies have found that mysid diets were dominated by phytoplankton like diatoms and dinoflagellates (Chew et al., 2012, Omweri et al., 2021). Conversely, Focke & Mees (1999) found that copepods, rotifers, and cladocerans were the most common diet items in several European estuaries, even in the spring. Differences between that study and ours may be due to their use of microscopy and visual identification of prey parts to identify mysid stomach contents. There is a chance that ingestion and digestion may have degraded some prey items to unidentifiable levels.

Experimental studies support that mysids exhibit preferences for certain types of prey depending on the energy required for capture, or the availability of different types of prey (Bowers & Grossnickle 1978, Kouassi et al., 2006, Wilhelm et al., 2002, Carrasco et al., 2007, Griffin et al., 2020). Preferences tend to lean toward larger animal prey over smaller prey for *T. Chiltoni* in laboratory experiments (Wilhelm et al., 2002). *L. benedini* preferred phytoplankton over animal prey in the field (Hanselmann et al., 2013). Griffin et al. (2020) claim that *M. relicta* balance foraging energy and nutritional value. They hypothesized that mysids would consume the cladoceran *Daphnia* over detritus when presented with both in experiments. Their findings suggest true omnivory, as experimental mysids readily consumed both *Daphnia* and detritus. We could not estimate prey preference of mysids in this study, because we did not have estimates of abundance of the prey field in our sampling locations. It has also been shown that some mysids exhibit prey preferences for phytoplankton over vascular plants *in situ* (Chew et al., 2012). Our findings align with this, because we found few sequences associated with vascular plants (aquatic or otherwise) and many sequences associated with phytoplankton. However, the lower presence of vascular plants may also be due to marker choice in the amplification of extracted DNA in both studies (Creer et al. 2016).

Mysid Diet Methodology

Several methods have historically been used to identify stomach contents of mysids. The most common methods have been visual observation under microscopes and using stable isotope composition. Microscopy, while typically readily available, requires identifiable material in the stomach contents, which is not always feasible with such small organisms. Even when preservation of the stomach contents is used, one must be able to identify the small, potentially fragmented plants, animals, phytoplankton, and detrital matter, which often requires special equipment and taxonomic expertise. Rudstam et al. (1989) used gut fluorescence in addition to microscopy to characterize the prey of mysid stomachs, which is useful for identifying algal components of the diet, but does not help with animal parts. Bulk stable isotope analysis is useful for understanding what generally makes up the diet of an organism, and from what habitats they originate, but it relies on the amount of potential prey contributing to diets. DNA metabarcoding is becoming more popular for diet studies because it can identify prey to low taxonomic levels even when digestion has taken place (Pagenkopp Lohan et al., 2023). Like visual methods, DNA metabarcoding only provides a snapshot of what has recently been consumed by the consumer organism, but it is powerful because it can do so without identifiable body parts of the prey, unlike microscopy. To date, we are only aware of two studies that have used molecular methods to better understand the diets of mysids. Gorokhova (2009) used PCR to detect a specific prey type (*Nodularia* spp.) in the stomach contents and fecal pellets of *M. relicta* and *M. mixta*. While DNA was successfully amplified from stomach contents and fecal pellets, Gorokhova (2009) found a higher frequency of amplification in mysid stomach samples compared to fecal pellet samples. While Gorokhova (2009) targeted a singular type of cyanobacteria, this may justify the use of stomach contents in our own study. Nakamura et al. (2020) used a combination of

microscopy, stable isotope signatures, and DNA metabarcoding to identify the prey and trophic level of *N. awatschensis* in Lake Kasumigaura, Japan. Their DNA metabarcoding differed from ours mainly because they 1) sampled from a freshwater lake in Japan 2) used the fecal pellets of mysids rather than the stomachs, and 3) digested their samples at a higher temperature for less time during extraction. They also used a Peptide Nucleic Acid (PNA) specific to *N. awatschensis* that would attempt to suppress amplification of sequences detected as the consumer mysids on one set of their PCR samples (the other set used no attempt to block sequences). Their use of a PNA successfully suppressed some mysid sequences, leading to 30-50% lower *N. awatschensis* sequences, compared to their samples without PNA. Similar to our study, they fixed samples in ethanol and amplified the 18S ribosomal DNA. Nakamura et al. (2020) found similar prey types as we did, with most of their sequences (after mysids) belonging to diatoms (Bacillariophyta) and green algae (Chlorophyta and Charophyta). They also identified copepods in metabarcoding, but copepods were not frequent or abundant. This is similar to our study, which was dominated by diatoms, dinoflagellates, and green algae.

GAM variables

We used GAMs to analyze the impacts of various predictor variables on the presence of ASVs in the Patuxent River, the relationship between consumer length and putative prey length, and the effects of different predictors on the abundance of ASV counts. The GAM for the presence of prey was only in the Patuxent River's mysid-excluded data since all other datasets had inconsistent presence of prey ASVs. We found that length was the sole best predictor for the presence of prey ASVs in our Patuxent sites, which may be due to there being a higher volume of stomach contents from samples that contained larger mysids. There was no relationship between the size of the consumer mysids and the size of prey consumed for any of the St. Marys

samples, or for the mysid-excluded Patuxent River samples. This means that mysids of varying sizes were consuming relatively similar sized prey. This is reasonable, since most of our prey ASVs were identified as a type of microalgae or protist, which can be consumed by most mysids whole (Figure 2.3; Grossnickle 1982, Takahashi et al., 2015), and do not necessarily have size-distinct life stages as they mature (Spaulding et al., 2021). For mysid-included Patuxent samples, we saw that larger mysids were more likely to consume smaller prey, which may just be a result of most of the smaller consumer mysids being dominated by mysid ASVs, and therefore less variable than the diets of the larger mysids. We also wanted to understand which of our predictor variables might influence the amount of ASV sequences for potential future studies and to understand potential impacts of our sampling. Our GAMs for St. Marys River suggested that the sites were the best predictor for the general abundance of ASV sequences, where site 1 had higher sequence abundances. Site 1 was sampled about three hours before site 2, so the disparities may be due to our mysids having consumed and retained more earlier in the day with mysids caught later on may have already evacuated some of the material by the time of capture. Mysid lengths and the time of sampling were significantly associated with higher ASV sequences in the Patuxent River with larger mysids and those caught in our morning samples (temporally later) had higher abundances. Lengths being a significant factor could be due to a higher volume of stomach contents to extract from and amplify prey DNA. Sampling time being another significant factor could also be due to when mysids are consuming prey relative to when they were captured. For Patuxent River mysid included data, water column position was another significant factor, which could be due to the distinctions in behaviors of mysids of varying sizes typically being associated with different depths in the water column (Gorokhova 2009).

Mysid Length and Trophic Levels

The mysids in our study were between 2.49 and 10.32 mm in length (Table A2.1). We found that larger mysids consumed a wider variety of prey items. This may be due to either a detection effect or differences in diet. Stomachs from larger mysids should contain a higher volume of material, which would provide more DNA to amplify. Smaller mysids have been found to consume less prey that is smaller and more rapidly evacuated, which may mean that their gut contents were evacuated more quickly (Bowers & Grossnickle 1978, Grossnickle 1982, Johnston & Lasenby 1982, Fockedey & Mees 1999, Hrycik et al., 2015, Evans et al., 2018). Smaller individuals also tend to have higher metabolic rates, digesting their prey more rapidly. Mysid diets also change ontogenetically, with many larger mysids found to consume higher volumes and more types of prey (Fockedey & Mees 1999, Johannsson et al., 2001, Evans et al., 2018). Grossnickle (1982) and Takahashi et al. (2015) found that as *M. relicta* and *Neomysis mirabilis* grow, they are more likely to consume different types of prey and are may be limited in what they can consume until they reach certain stages of life. Similarly, Quillen et al. (2022) found that larger *N. americana* in the Choptank River of Chesapeake Bay generally occupied higher trophic positions when a variety of prey were present. Rudstam et al. (1989) and Gorokhova (2009) found that smaller, younger mysids are more likely to be higher in the water column than larger mysids, which may provide them with access to different types of prey altogether. Spatial differences in habitat use with size could explain why water column and mean mysid length were identified as important variables for explaining the abundance of sequences in our Patuxent River mysid-included samples.

Parasitism

We were unable to tell whether an ASV identified in our samples was prey, secondary prey (i.e., prey of the prey), or a parasite, which can occur in DNA metabarcoding studies (Bowser et al., 2013). Several genera in our samples contain parasitic species including the fungus genera *Arkaya* and *Pythiaceae*, the protist genera *Zoothamnium*, *Protapsa*, *Gregarina*, *Cephaloidophora*, *Mychonastes*, and *Hyalophysa*, and the dinoflagellate genus *Yihiella* (File S1). Mysids may have consumed parasites that were present in their prey, as many types of zooplankton act as intermediate hosts for parasites of larger organisms (Lozano-Cobo et al., 2017), including mysids (Jackson et al., 1997). Much of the literature on mysid parasitism emphasizes isopods and copepods as common parasites (Daly & Damkaer 1986, Heron & Damkaer 1986, Shimomura et al., 2005, Ohtsuka et al., 2007). However, we found no evidence of isopods in our samples, and the copepods did not belong to parasitic genera. Existing studies of internal parasites are quite limited for mysids. Fernandez-Leborans (2004) reported parasitic protozoans of *M. relicta* in a Lithuanian lake that belonged to the genera *Vorticella*, *Dendrosoma* and *Tokophrya*; but none of these were found in our samples (Table 2.1). Calanoid copepods have been found to have protists and ciliates within them, which may be parasitic depending on the species, and would be present in mysid stomachs if their host was consumed (Yeh et al., 2020). However, the species found by Yeh et al. (2020), *Ganymedes apsteini*, was not identified in any of our samples, nor any ASVs assigned to the same genus.

Secondary Prey

Some of the identified taxa may have been present due to secondary predation. The most abundant heterotrophs that were identified in our samples were copepods, whose diets are also wide ranging and overlap with what we found within mysids, especially in terms of

phytoplankton, smaller zooplankton, and protists (Gowing & Wishner 1992, Friedland et al., 2016, Yeh et al., 2020, Holmes & Kimmerer 2022, Chae et al., 2023, Flo et al., 2024). Therefore, some phytoplankton taxa in our samples may have been ingested by copepods before the copepods were eaten by mysids. Copepod sequence abundance was positively correlated with sequence abundances of macroalgae, microalgae, and protists in our Patuxent River samples, making us unable to rule out secondary predation as a potential source of uncertainty in this study. Other studies discounted the likelihood of secondary predation due to the rapid evacuation that copepods undergo upon consuming food (Dam and Peterson 1988, Gorokhova 2009). Also, pennate diatoms have previously been identified in the stomach contents of mysids, separate from copepods, and not masticated (Personal Communication R. Woodland 2025). Had the diatoms been initially consumed by mysids, mastication would have likely been more noticeable (Personal Communication R. Woodland 2025).

Mysid Digestion and Evacuation

Evacuation or digestion rates of an organism should be considered to some degree in diet studies, as prey that are consumed eventually get metabolized or excreted. The amplified DNA that was sequenced in our study was likely consumed relatively close to the time of collecting the mysids from the field. Mysid evacuation rates were calculated to be approximately 1 hour by Focke & Mees (1999), but Rudstam et al. (1989) found evidence of food in their stomachs for up to 13 hours. Gorokhova (2009) found cyanobacteria in the stomachs of mysids up to 8 hours after consumption. For our results, this means that the putative prey may only be representative of what mysids ingest close to our sampling time periods. This time frame supports the use of DNA metabarcoding because stomach contents may be present but degraded after a certain

amount of time. The ability to identify somewhat digested material, without having to rely on maintained parts or shape of a prey organism then becomes very useful in these instances.

Tag-Jumping

We separated the data into mysid-excluded and mysid-included sets. In our mysid-included sets, we had instances of non-consumer mysid taxa in many of the samples. The likelihood of this being due to consumption of these non-consumer mysids is low, as in our sampling, all of the mysids from St. Marys were *Americamysis*, and most from the Patuxent were *N. americana*, with few *Americamysis* individuals. The presence of the non-consumer mysid sequences may be due to a phenomenon known as “tag-jumping” that takes place when the amplicons tagged in indexing take on other incorrect tags (Schnell et al., 2015). It is not uncommon in high throughput sequencing studies such as ours (Schnell et al., 2015). The abundance of these potentially “tag-jumped” sequences can help to determine if they were actually consumed, or mismatched in detection. We plan on looking further into the relative abundance of these non-consumer mysid sequences.

General Assumptions

It is likely that DNA of some taxa present in the mysid stomachs was not amplified, as the PCR process for amplification is random and may not evenly amplify the sequences in each sample. Krehenwinkel et al. (2017) suggested that amplification bias often takes place in metabarcoding studies, and is typically linked to amplicon length variation, the locus of the DNA strand being targeted, or the amount of PCR cycling. This means that our study is conservative in representing the diversity of taxa that mysids are consuming *in situ* in the St. Marys and Patuxent rivers. Our sampling was very limited, both spatially and temporally. This likely means that we

did not observe the full range of what mysids may be consuming *in situ* within these habitats or rivers. We also sampled only in the relatively shallow benthic habitat for St. Marys and the upper water column for Patuxent, meaning that there are vertical habitats missing from both studies, as well as a lack of representation from any deep channel mysids. This limits our conclusions about mysids across habitats of Chesapeake Bay. Our sampling of each river took place within a 24-hour period, with sites being sampled within hours of one another. This means that we were unable to make inferences about the seasonal, diel, or overall temporal shifts in stomach contents of mysids beyond the few hours sampled for each tributary.

Conclusions

We successfully identified potential prey items of *N. americana* and *Americamysis* spp. in the St. Marys and Patuxent Rivers. *Neomysis americana* and *Americamysis* spp. appeared to be generalist omnivores that relied more on phytoplankton prey than zooplankton or other taxa during the sampling period. Because mysids are thought to be important connectors of energy and nutrients in marine and aquatic systems, understanding their diets is important for characterizing their role in the ecosystem. Most previous studies of mysid diets used microscopy and stable isotopic signatures to identify the prey of mysids and their trophic contributions in ecosystems. DNA metabarcoding provides a powerful new tool for understanding food webs, particularly for organisms like mysids, where visual identification of prey in gut contents is challenging.

Tables

Table 2.1. Unique amplicon sequence variants (ASVs), genus, common name, microalgae type and abundance of the ASV in all samples combined from the St. Marys and Patuxent Rivers.

ASV Number	Genus	Type	Microalgae Type	Total Frequency
Seq1	<i>Neomysis</i>	Mysid	–	5358849
Seq2	<i>Americamysis</i>	Mysid	–	761306
Seq3	<i>Americamysis</i>	Mysid	–	135232
Seq4	<i>Neomysis</i>	Mysid	–	12926
Seq5	<i>Americamysis</i>	Mysid	–	12312
Seq6	<i>Neomysis</i>	Mysid	–	11866
Seq7	<i>Nais</i>	Annelid	–	11444
Seq8	<i>Acartia</i>	Copepod	–	4399
Seq9	<i>Canuella</i>	Copepod	–	3665
Seq10	<i>Neomysis</i>	Mysid	–	3594
Seq11	<i>Neomysis</i>	Mysid	–	2711
Seq12	<i>Neomysis</i>	Mysid	–	1706
Seq13	<i>Neomysis</i>	Mysid	–	1599
Seq14	<i>Neomysis</i>	Mysid	–	1056
Seq15	<i>Neomysis</i>	Mysid	–	943
Seq16	<i>Neomysis</i>	Mysid	–	912
Seq17	<i>Neomysis</i>	Mysid	–	788
Seq18	<i>Neomysis</i>	Mysid	–	706
Seq19	<i>Americamysis</i>	Mysid	–	595
Seq20	<i>Americamysis</i>	Mysid	–	537
Seq21	<i>Tachidius</i>	Copepod	–	489
Seq22	<i>Neomysis</i>	Mysid	–	415

Seq23	<i>Neomysis</i>	Mysid	–	395
Seq24	<i>Cyclotella</i>	Microalgae	Diatom	393
Seq25	<i>Neomysis</i>	Mysid	–	350
Seq26	<i>Tenualosa</i>	Finfish	–	335
Seq27	<i>Neomysis</i>	Mysid	–	326
Seq28	<i>Neomysis</i>	Mysid	–	273
Seq29	<i>Neomysis</i>	Mysid	–	190
Seq30	<i>Americamysis</i>	Mysid	–	254
Seq31	<i>Cyclotella</i>	Microalgae	Diatom	230
Seq32	<i>Gymnodinium</i>	Microalgae	Dinoflagellate	198
Seq33	<i>Neomysis</i>	Mysid	–	194
Seq34	<i>Arkaya</i>	Fungi	–	175
Seq35	<i>Prorocentrum</i>	Microalgae	Dinoflagellate	168
Seq36	<i>Americamysis</i>	Mysid	–	151
Seq37	<i>Neomysis</i>	Mysid	–	131
Seq38	<i>Neomysis</i>	Mysid	–	126
Seq39	<i>Acartia</i>	Copepod	–	117
Seq41	<i>Mataza</i>	Protist	–	92
Seq42	<i>Monodus</i>	Microalgae	Green Algae	85
Seq43	<i>Gregarina</i>	Protist	–	80
Seq44	<i>Navicula</i>	Microalgae	Diatom	78
Seq45	<i>Nais</i>	Annelid	–	78
Seq46	<i>Molgula</i>	Tunicate	–	77
Seq47	<i>Picochlorum</i>	Microalgae	Green Algae	60
Seq48	<i>Americamysis</i>	Mysid	–	58

Seq49	<i>Neomysis</i>	Mysid	–	55
Seq50	<i>Colpodella</i>	Protist	–	53
Seq51	<i>Desmodesmus</i>	Microalgae	Green Algae	44
Seq52	<i>Protaspis</i>	Protist	–	41
Seq53	<i>Cephaloidophora</i>	Protist	–	38
Seq54	<i>Neomysis</i>	Mysid	–	36
Seq55	<i>Parathalestris</i>	Copepod	–	35
Seq56	<i>Zoothamnium</i>	Protist	–	35
Seq57	<i>Americamysis</i>	Mysid	–	34
Seq58	<i>Myrica</i>	Terrestrial Plant	–	34
Seq59	<i>Prorocentrum</i>	Microalgae	Dinoflagellate	33
Seq60	<i>Navicula</i>	Microalgae	Diatom	33
Seq61	<i>Thalassiosira</i>	Microalgae	Diatom	29
Seq62	<i>Acer</i>	Terrestrial Plant	–	29
Seq63	<i>Neomysis</i>	Mysid	–	29
Seq64	<i>Neomysis</i>	Mysid	–	29
Seq65	<i>Picochlorum</i>	Microalgae	Green Algae	27
Seq66	<i>Hyalophysa</i>	Protist	–	26
Seq67	<i>Pythiaceae</i>	Fungi	–	25
Seq68	<i>Colpodella</i>	Protist	–	23
Seq69	<i>Minidiscus</i>	Microalgae	Diatom	22
Seq71	<i>Americamysis</i>	Mysid	–	20
Seq72	<i>Yihiella</i>	Microalgae	Dinoflagellate	18
Seq73	<i>Tachidius</i>	Copepod	–	18
Seq74	<i>Americamysis</i>	Mysid	–	16

Seq75	<i>Phagomyxa</i>	Protist	–	13
Seq76	<i>Mychonastes</i>	Microalgae	Green Algae	12
Seq77	<i>Protaspa</i>	Protist	–	11
Seq78	<i>Neomysis</i>	Mysid	–	11
Seq79	<i>Melosira</i>	Microalgae	Diatom	11
Seq80	<i>Hydractinia</i>	Hydrozoan	–	11
Seq81	<i>Neomysis</i>	Mysid	–	11
Seq82	<i>Biddulphia</i>	Macroalgae	–	10
Seq83	<i>Choricystis</i>	Microalgae	Green Algae	10
Seq84	<i>Arkaya</i>	Fungi	–	9
Seq85	<i>Mataza</i>	Protist	–	8
Seq86	<i>Protaspis</i>	Protist	–	8
Seq87	<i>Gymnodinium</i>	Microalgae	Dinoflagellate	6

Figures

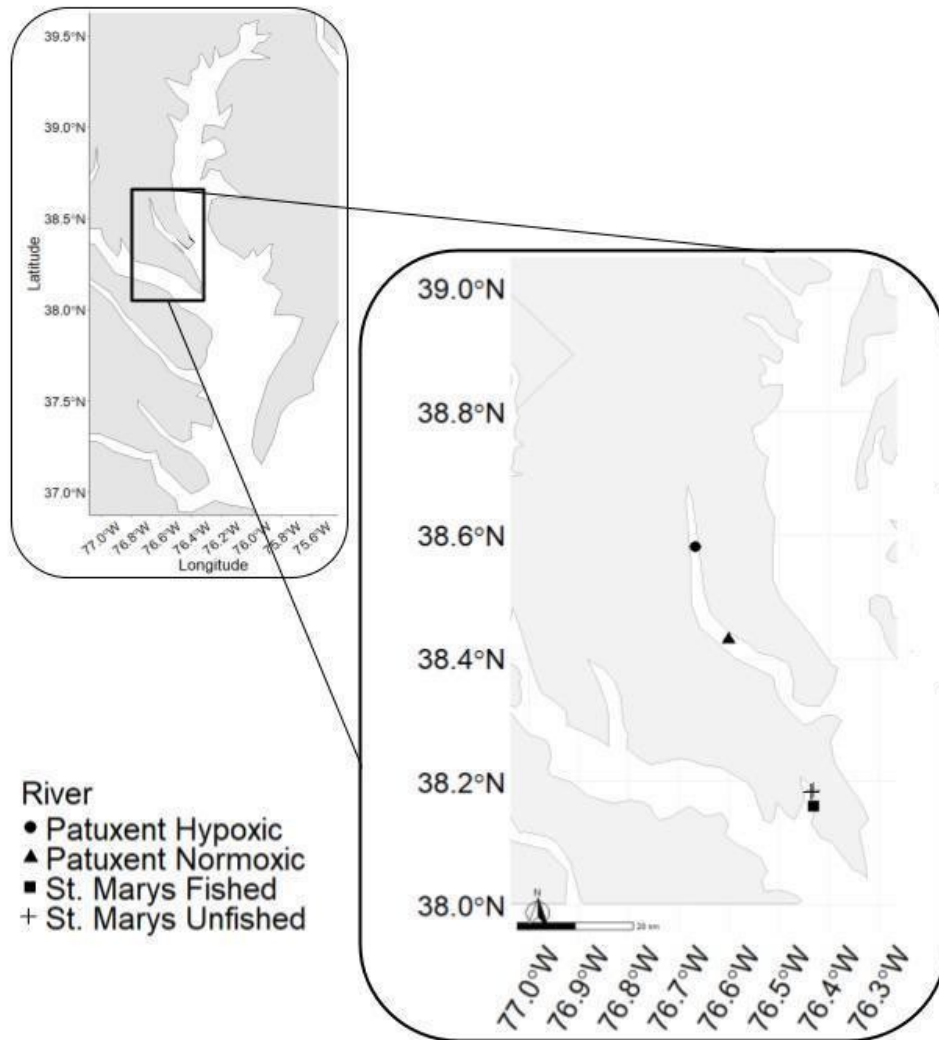


Figure 2.1. Sampling sites in the St. Marys River and Patuxent River, Maryland. Patuxent Hypoxic is Patuxent Site 2, and Patuxent Normoxic is Patuxent site 5 in the text. St. Marys Fished is St. Marys site 1, and St. Marys Unfished is St. Marys site 2 in the text.

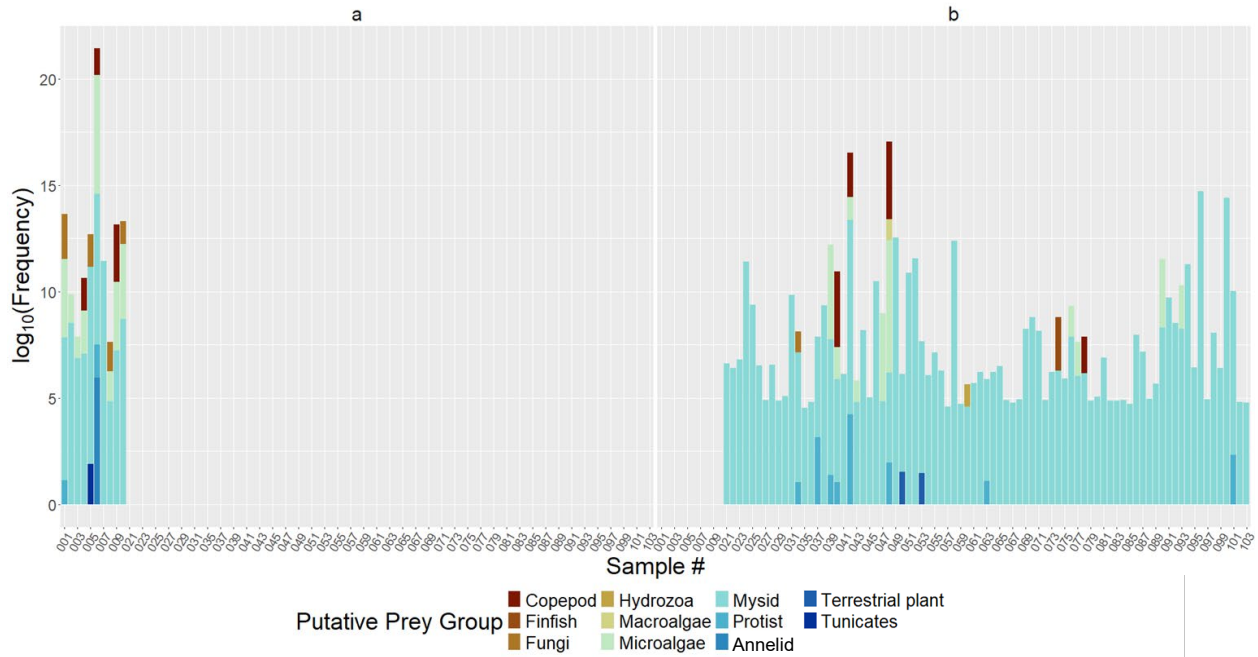


Figure 2.2. Logarithm (base 10) of abundance of sequences by sampling site and ASV groups from the a) St. Marys River and b) Patuxent River, Maryland. The sample IDs are on the x-axis.

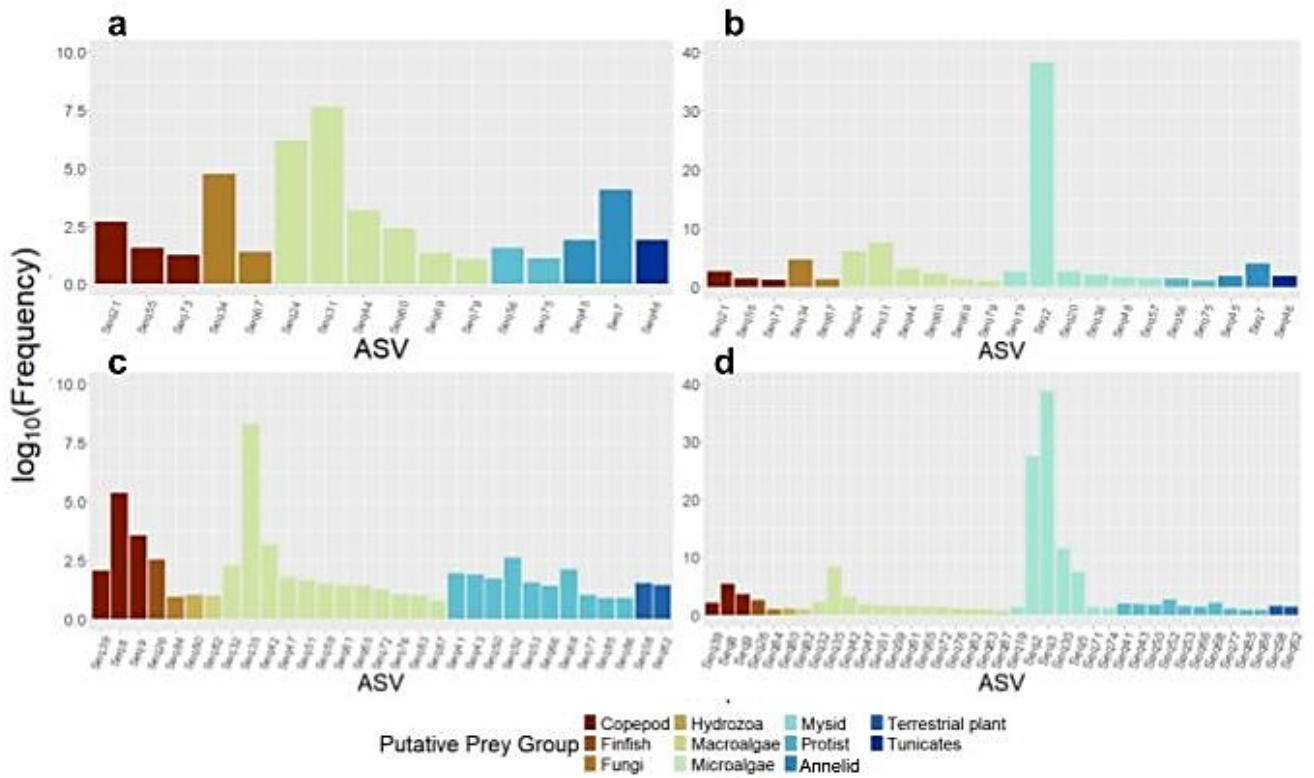


Figure 2.3. Frequency (log₁₀-scale) of amplicon sequence variants (ASVs) for taxa identified in the a) *St. Marys* mysid-excluded, b) *St. Marys* mysid-included, c) *Patuxent* mysid-excluded, and d) *Patuxent* mysid-included sequences. The scales of the y-axis are 0–10 for the mysid-excluded sequences, and 0–40 for the mysid-included sequences. ASVs are described in Table 1.

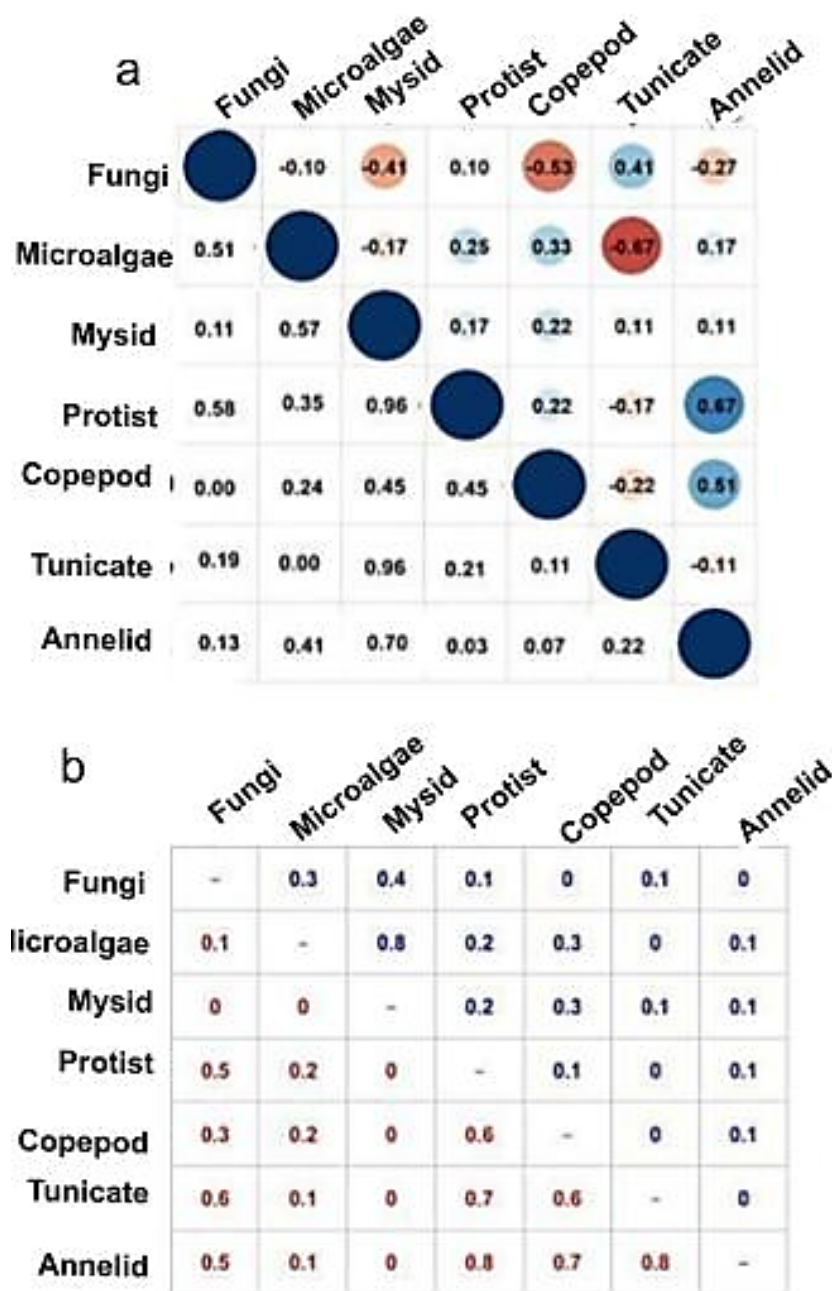


Figure 2.4. a) Pearson correlations for binary data of the presence of the ASV groups in the Patuxent River and b) the co-occurrences and co-absences of prey groups. In panel a, the circle color represents the sign of the correlation, with warmer colored circles being negative correlations and cooler colored circles being positive correlations. Circle sizes indicate the strength of the correlations. P-values of each correlation (not corrected for multiple comparisons) are in the lower diagonal matrix.

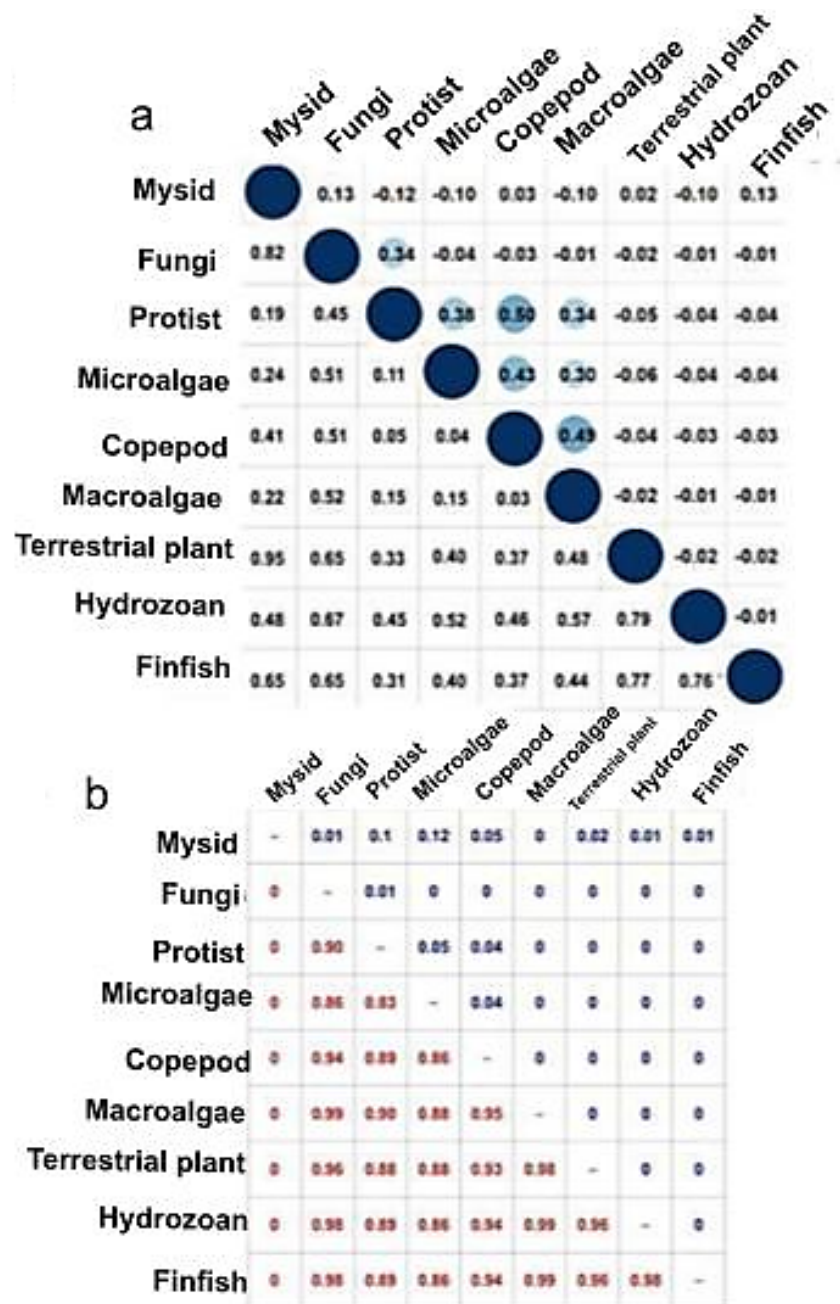


Figure 2.5. a) Pearson correlations for binary data of the presence of the ASV groups in the Patuxent River and b) the co-occurrences and co-absences of prey groups. In panel a, the circle color represents the sign of the correlation, with warmer colored circles being negative correlations and cooler colored circles being positive correlations. Circle sizes indicate the strength of the correlations. P-values of each correlation (not corrected for multiple comparisons) are in the lower diagonal matrix.

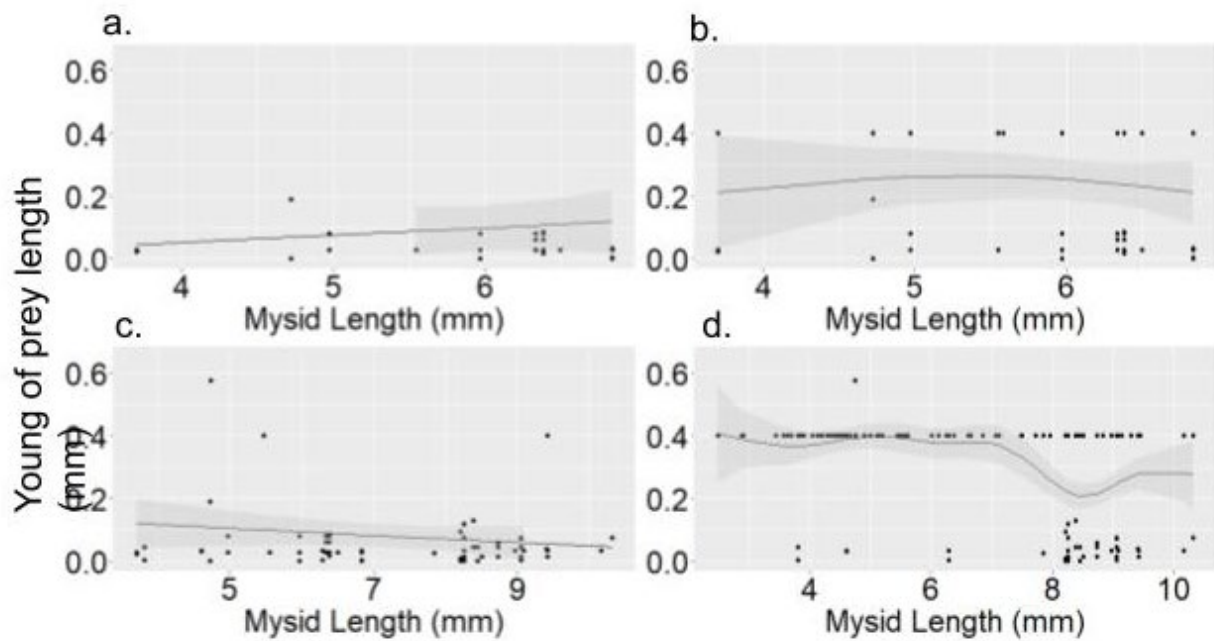


Figure 2.6. Estimated generalized additive model relationships between mean mysid length in a sample and length of the young of prey of taxa identified using DNA metabarcoding for a) *St. Marys mysid* excluded, b) *St. Marys mysid* included, c) *Patuxent mysid*-excluded, and d) *Patuxent mysid*-included samples. The black lines represent the estimated relationships, the black points are the data, and the grey shaded areas are the 95% confidence intervals.

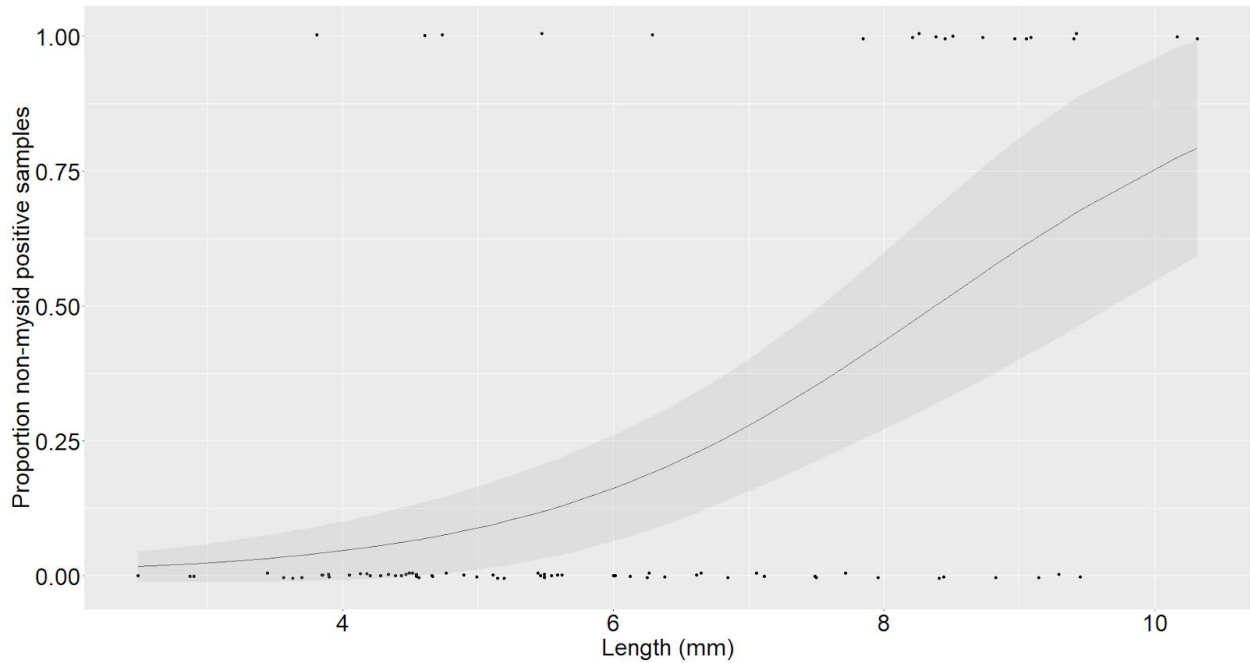


Figure 2.7. Proportion of mysid stomach samples with non-mysid taxa identified using DNA metabarcoding for the Patuxent River as a function of length. The predicted presence is represented by the black line with 95% confidence intervals in grey. Points include a random jitter to reduce overlap.

References

- Borza, P., Duleba, M., & Egri, Á. (2023). Filter feeding in the mysid crustacean *Limnomysis benedeni*: Evidence of the maxillary pump and the ventral filtration current. *Zoologischer Anzeiger*, 302, 260–265. <https://doi.org/10.1016/j.jcz.2023.01.002>
- Bowers, J. A., & Grossnickle, N. E. (1978). The Herbivorous Habits of *Mysis relicta* in Lake Michigan. *Limnology and Oceanography*, 23, 767–776. <https://doi.org/10.4319/lo.1978.23.4.0767>
- Bowser, A. K., Diamond, A. W., & Addison, J. A. (2013). From Puffins to Plankton: A DNA-Based Analysis of a Seabird Food Chain in the Northern Gulf of Maine. *PloS One*, 8, 83152–83152. <https://doi.org/10.1371/journal.pone.0083152>
- Bråte, J., Logares, R., Berney, C., Ree, D. K., Klaveness, D., Jakobsen, K. S., & Shalchian-Tabrizi, K. (2010). Freshwater Perkinsea and marine-freshwater colonizations revealed by pyrosequencing and phylogeny of environmental rDNA. *The ISME Journal*, 4, 1144–1153. <https://doi.org/10.1038/ismej.2010.39>
- Caldwell, T. J., Wilhelm, F. M., & Dux, A. (2016). Non-native pelagic macroinvertebrate alters population dynamics of herbivorous zooplankton in a large deep lake. *Canadian Journal of Fisheries and Aquatic Sciences*, 73, 832–843. <https://doi.org/10.1139/cjfas-2015-0144>
- Callahan, B. J., McMurdie, P. J., Rosen, M. J., Han, A. W., Johnson, A. J. A., & Holmes, S. P. (2016). DADA2: High-resolution sample inference from Illumina amplicon data. *Nature Methods*, 13, 581–583. <https://doi.org/10.1038/nmeth.3869>
- Carrasco, N. K., Perissinotto, R., & Miranda, N. A. F. (2007). Effects of silt loading on the feeding and mortality of the mysid *Mesopodopsis africana* in the St. Lucia Estuary, South

- Africa. *Journal of Experimental Marine Biology and Ecology*, 352, 152–164.
<https://doi.org/10.1016/j.jembe.2007.07.006>
- Cartes, J. E., & Sorbe, J. C. (1998). Aspects of population structure and feeding ecology of the deep-water mysid *Boreomysis arctica*, a dominant species in western Mediterranean slope assemblages. *Journal of Plankton Research*, 20, 2273–2290.
<https://doi.org/10.1093/plankt/20.12.2273>
- Chae, Y.-J., Oh, H.-J., Kwak, I.-S., Chang, K.-H., & Jo, H. (2023). A study of the feeding characteristics of a small and medium-sized copepod species (*Sinocalanus tenellus*) using genetic analysis techniques: seasonal comparison of potential/eaten food sources focused on phytoplankton. *Frontiers in Marine Science*, 10.
<https://doi.org/10.3389/fmars.2023.1234754>
- Chew, L. L., Chong, V. C., Tanaka, K., & Sasekumar, A. (2012). Phytoplankton fuel the energy flow from zooplankton to small nekton in turbid mangrove waters. *Marine Ecology Progress Series*, 469, 7–24. <https://doi.org/10.3354/meps09997>
- Cowles, R. P. (1930). A biological study of the offshore waters of Chesapeake Bay. *Bull. Bur. Fish. Wash*, 46, 277–381.
- Creer, S., Deiner, K., Frey, S., Porazinska, D., Taberlet, P., Thomas, W. K., Potter, C., Bik, H. M., & Freckleton, R. (2016). The ecologist's field guide to sequence-based identification of biodiversity. *Methods in Ecology and Evolution*, 7, 1008–1018.
<https://doi.org/10.1111/2041-210x.12574>
- Dam, H. G., & Peterson, W. T. (1988). The effect of temperature on the gut clearance rate constant of planktonic copepods. *Journal of Experimental Marine Biology and Ecology*, 123, 1–14. [https://doi.org/10.1016/0022-0981\(88\)90105-0](https://doi.org/10.1016/0022-0981(88)90105-0)

- Daly, K. L., & Damkaer, D. M. (1986). Population dynamics and distribution of *Neomysis mercedis* and *Alienacanthomysis macropsis* (Crustacea: Mysidacea) in relation to the parasitic copepod *Hansenulus trebax* in the Columbia River estuary. *J. Crustacean Biol.*, 6, 840–857. <https://doi.org/10.2307/1548396>
- Dean, A. F., Bollens, S. M., Simenstad, C., & Cordell, J. (2005). Marshes as sources or sinks of an estuarine mysid: demographic patterns and tidal flux of *Neomysis kadiakensis* at China Camp marsh, San Francisco estuary. *Estuarine, Coastal and Shelf Science*, 63, 1–11. <https://10.1016/j.ecss.2004.08.019>
- Dollive, S., Peterfreund, G. L., Sherrill-Mix, S., Bittinger, K., Sinha, R., Hoffmann, C., Nabel, C. S., Hill, D. A., Artis, D., Bachman, M. A., Custers-Allen, R., Grunberg, S., Wu, G. D., Lewis, J. D., & Bushman, F. D. (2012). A tool kit for quantifying eukaryotic rRNA gene sequences from human microbiome samples. *Genome Biology*, 13, Article R60. <https://doi.org/10.1186/gb-2012-13-7-r60>
- Evans, T. M., Naddafi, R., Weidel, B. C., Lantry, B. F., Walsh, M. G., Boscarino, B. T., Johannsson, O. E., & Rudstam, L. G. (2018). Stomach contents and stable isotopes analysis indicate *Hemimysis anomala* in Lake Ontario are broadly omnivorous. *Journal of Great Lakes Research*, 44, 467–475. <https://doi.org/10.1016/j.jglr.2018.03.003>
- Fernandez-Leborans, G. (2004). Protozoan epibionts on *Mysis relicta* Loven, 1862 (Crustacea, Mysidacea) from Lake Lūšiai (Lithuania). *Acta Zoologica*, 85, 101–112. <https://doi.org/10.1111/j.0001-7272.2004.00162.x>
- Flo, S., Svensen, C., Præbel, K., Bluhm, B. A., & Vader, A. (2024). Dietary plasticity in small Arctic copepods as revealed with prey metabarcoding. *Journal of Plankton Research*, 46, 500–514. <https://doi.org/10.1093/plankt/fbae042>

- Fockedeey, N., & Mees, J. (1999). Feeding of the hyperbenthic mysid *Neomysis integer* in the maximum turbidity zone of the Elbe, Westerschelde and Gironde estuaries. *Journal of Marine Systems*, 22, 207–228. [https://doi.org/10.1016/S0924-7963\(99\)00042-1](https://doi.org/10.1016/S0924-7963(99)00042-1)
- Friedland, K. D., Record, N. R., Asch, R. G., Kristiansen, T., Saba, V. S., Drinkwater, K. F., Henson, S., Leaf, R. T., Morse, R. E., Johns, D. G., Large, S. I., Hjøllø, S. S., Nye, J. A., Alexander, M. A., & Ji, R. (2016). Seasonal phytoplankton blooms in the North Atlantic linked to the overwintering strategies of copepods. *Elementa (Washington, D.C.)*, 4. <https://doi.org/10.12952/journal.elementa.000099>
- Gallegos, C. L., & Jordan, T. E. (2002). Impact of the spring 2000 phytoplankton bloom in Chesapeake Bay on optical properties and light penetration in the Rhode River, Maryland. *Estuaries*, 25, 508–518. <https://doi.org/10.1007/bf02804886>
- Gorokhova, E. (2009). Toxic cyanobacteria *Nodularia spumigena* in the diet of Baltic mysids: Evidence from molecular diet analysis. *Harmful Algae*, 8, 264–272. <https://doi.org/10.1016/j.hal.2008.06.006>
- Gowing, M. M., & Wishner, K. F. (1992). Feeding ecology of benthopelagic zooplankton on an eastern tropical Pacific seamount. *Marine Biology*, 112, 451–467. <https://doi.org/10.1007/bf00356291>
- Griffin, J. E., O'Malley, B. P., & Stockwell, J. D. (2020). The freshwater mysid *Mysis diluviana* (Audzijonyte & Väinölä, 2005) (Mysida: Mysidae) consumes detritus in the presence of *Daphnia* (Cladocera: Daphniidae). *Journal of Crustacean Biology*, 40, 520–525. <https://doi.org/10.1093/jcbiol/ruaa053>
- Grossnickle, N. E. (1982). Feeding habits of *Mysis relicta*? an overview. *Hydrobiologia*, 93, 101–107. <https://doi.org/10.1007/BF00008103>

- Guillou, L., Bachar, D., Audic, S., Bass, D., Berney, C., Bittner, L., Boutte, C., Burgaud, G., de Vargas, C., Decelle, J., del Campo, J., Dolan, J. R., Dunthorn, M., Edvardsen, B., Holzmann, M., Kooistra, W. H. C. F., Lara, E., Le Bescot, N., Logares, R., ... Christen, R. (2013). The Protist Ribosomal Reference database (PR2): a catalog of unicellular eukaryote Small Sub-Unit rRNA sequences with curated taxonomy. *Nucleic Acids Research*, *41*, 597–604. <https://doi.org/10.1093/nar/gks1160>
- Hagenbüchle, O., Santer, M., Steitz, J. A., & Mans, R. J. (1978). Conservation of the primary structure at the 3' end of 18S rRNA from eucaryotic cells. *Cell*, *13*, 551–563. [https://doi.org/10.1016/0092-8674\(78\)90328-8](https://doi.org/10.1016/0092-8674(78)90328-8)
- Hanselmann, A. J., Hodapp, B., & Rothhaupt, K.-O. (2013). Nutritional ecology of the invasive freshwater mysid *Limnomysis benedeni*: field data and laboratory experiments on food choice and juvenile growth. *Hydrobiologia*, *705*, 75–86. <https://doi.org/10.1007/s10750-012-1382-8>
- Heron, G. A., & Damkaer, D. M. (1986). A new nicothoid copepod parasitic on mysids from northwestern North America. *J. Crustacean Biol*, *6*, 652–665. <https://doi.org/10.2307/1548379>
- Holmes, A. E., & Kimmerer, W. J. (2022). Phytoplankton prey of an abundant estuarine copepod identified *in situ* using DNA metabarcoding. *Journal of Plankton Research*, *44*, 316–332. <https://doi.org/10.1093/plankt/fbac002>
- Hrycik, A. R., Simonin, P. W., Rudstam, L. G., Parrish, D. L., Pientka, B., & Mihuc, T. B. (2015). Mysis zooplanktivory in Lake Champlain: A bioenergetics analysis. *Journal of Great Lakes Research*, *41*, 492–501. <https://doi.org/10.1016/j.jglr.2015.03.011>

- Jackson, C. J., Marcogliese, D. J., & Burt, M. D. (1997). Role of hyperbenthic crustaceans in the transmission of marine helminth parasites. *Canadian Journal of Fisheries and Aquatic Sciences*, 54, 815–820. <https://doi.org/10.1139/f96-329>
- Johannsson, O. E., Leggett, M. F., Rudstam, L. G., Servos, M. R., Mohammadian, M. A., Gal, G., Dermott, R. M., & Hesslein, R. H. (2001). Diet of *Mysis relicta* in Lake Ontario as revealed by stable isotope and gut content analysis. *Canadian Journal of Fisheries and Aquatic Sciences*, 58, 1975–1986. <https://doi.org/10.1139/f01-118>
- Johnston, N. T., & Lasenby, D. C. (1982). Diet and feeding of *Neomysis mercedis* Holmes (Crustacea, Mysidacea) from the Fraser River Estuary, British Columbia. *Canadian Journal of Zoology*, 60, 813–824. <https://doi.org/10.1139/z82-112>
- Kiljunen, M., Peltonen, H., Lehtiniemi, M., Uusitalo, L., Sinisalo, T., Norkko, J., Kunnasranta, M., Torniainen, J., Rissanen, A. J., & Karjalainen, J. (2020). Benthic-pelagic coupling and trophic relationships in northern Baltic Sea food webs. *Limnology and Oceanography*, 65, 1706–1722. <https://doi.org/10.1002/lno.11413>
- Kouassi, E., Pagano, M., Saint-Jean, L., & Sorbe, J. C. (2006). Diel vertical migrations and feeding behavior of the mysid *Rhopalophthalmus africana* (Crustacea: Mysidacea) in a tropical lagoon (Ebrié, Côte d'Ivoire). *Estuarine, Coastal and Shelf Science*, 67, 355–368. <https://doi.org/10.1016/j.ecss.2005.10.019>
- Krehenwinkel, H., Wolf, M., Lim, J. Y., Rominger, A. J., Simison, W. B., & Gillespie, R. G. (2017). Estimating and mitigating amplification bias in qualitative and quantitative arthropod metabarcoding. *Scientific Reports*, 7(1), Article 17668. <https://doi.org/10.1038/s41598-017-17333-x>

- Laprise, R., & Dodson, J. J. (1994). Environmental variability as a factor controlling spatial patterns in distribution and species diversity of zooplankton in the St. Lawrence Estuary. *Marine Ecology Progress Series*, 107, 67–81. <https://doi.org/10.3354/meps107067>
- Lehtiniemi, M., Viitasalo, M., & Kuosa, H. (2002). Diet Composition Influences the Growth of the Pelagic Mysid Shrimp, *Mysis Mixta* (Mysidacea). *Boreal Environment Research*, 7, 121–128.
- Lesutienė, J., Gorokhova, E., Gasiūnaitė, Z. R., & Razinkovas, A. (2008). Role of mysid seasonal migrations in the organic matter transfer in the Curonian Lagoon, south-eastern Baltic Sea. *Estuarine, Coastal and Shelf Science*, 80, 225–234. <https://doi.org/10.1016/j.ecss.2008.08.001>
- Lozano-Cobo, H., Gómez-Gutiérrez, J., Franco-Gordo, C., & Gómez del Prado-Rosas, M. del C. (2017). The discovery of acanthocephalans parasitizing chaetognaths. *Acta Parasitologica*, 62, 401–411. <https://doi.org/10.1515/ap-2017-0048>
- Martin, M. (2011). Cutadapt removes adapter sequences from high-throughput sequencing reads. *EMBnet.Journal*, 17, 10-. <https://doi.org/10.14806/ej.17.1.200>.
- Mauchline J. (1980). The biology of mysids. *The Biology of Mysids and Euphausiids*, 3–369. <https://doi.org/10.2307/3242454>
- Mayor, E. D., & Chigbu, P. (2018). Mysid shrimp dynamics in relation to abiotic and biotic factors in the coastal lagoons of Maryland, Mid-West Atlantic, USA. *Marine Biology Research*, 14, 621–636. <https://doi.org/10.1080/17451000.2018.1472384>
- Nakamura, Y., Tuji, A., Makino, W., Matsuzaki, S. S., Nagata, N., Nakagawa, M., & Takamura, N. (2020). Feeding ecology of a mysid species, *Neomysis awatschensis* in the Lake Kasumigaura : combining approach with microscopy, stable isotope analysis and DNA

metabarcoding. *Plankton & Benthos Research*, 15, 44–54.

<https://doi.org/10.3800/pbr.15.44>

Ohtsuka, S., Harada, S., Shimomura, M., Boxshall, G. A., Yoshizaki, R., Ueno, D., Nitta, Y., Iwasaki, S., Okawachi, H., & Sakakihara, T. (2007). Temporal partitioning: dynamics of alternating occupancy of a host microhabitat by two different crustacean parasites.

Marine Ecology Progress Series, 348, 261–272. <https://doi.org/10.3354/meps07096>

Oliveira, A. F., Marques, S. C., Pereira, J. L., & Azeiteiro, U. M. (2023). A review of the order mysida in marine ecosystems: What we know what is yet to be known. *Marine Environmental Research*, 188, 106019–106019.

<https://doi.org/10.1016/j.marenvres.2023.106019>

Omweri, J. O., Suzuki, K. W., Houki, S., Lavergne, E., Inoue, H., Yokoyama, H., & Yamashita, Y. (2021). Flexible herbivory of the euryhaline mysid *Neomysis awatschensis* in the microtidal Yura River estuary, central Japan. *Plankton & Benthos Research*, 16, 278–

291. <https://doi.org/10.3800/pbr.16.278>

Pagenkopp Lohan, K. M., Aguilar, R., DiMaria, R., Heggie, K., Tuckey, T. D., Fabrizio, M. C., & Ogburn, M. B. (2023). Juvenile Striped Bass consume diverse prey in Chesapeake Bay tributaries. *Marine and Coastal Fisheries*, 15. <https://doi.org/10.1002/mcf2.10259>

Quillen, K., Santos, N., Testa, J. M., & Woodland, R. J. (2022). Coastal hypoxia reduces trophic resource coupling and alters niche characteristics of an ecologically dominant omnivore.

Food Webs, 33, Article e00252. <https://doi.org/10.1016/j.fooweb.2022.e00252>

Rappé, K., Fockedey, N., Van Colen, C., Cattrijsse, A., Mees, J., & Vincx, M. (2011). Spatial distribution and general population characteristics of mysid shrimps in the Westerschelde

- estuary (SW Netherlands). *Estuarine, Coastal and Shelf Science*, 91, 187–197.
<https://doi.org/10.1016/j.ecss.2010.10.017>
- R Core Team (2024). R: A Language and Environment for Statistical Computing. R Foundation for Statistical Computing, Vienna, Austria. <https://www.R-project.org/>
- Richterich, P. (1998). Estimation of Errors in “Raw” DNA Sequences: A Validation Study. *Genome Research*, 8, 251–259. <https://doi.org/10.1101/gr.8.3.251>
- Rudstam, L. G., Danielsson, K., Hansson, S., & Johansson, S. (1989). Diel vertical migration and feeding patterns of *Mysis mixta* (Crustacea, Mysidacea) in the Baltic Sea. *Marine Biology*, 101, 43–52. <https://doi.org/10.1007/BF00393476>
- Schnell, I. B., Bohmann, K., & Gilbert, M. T. P. (2015). Tag jumps illuminated – reducing sequence-to-sample misidentifications in metabarcoding studies. *Molecular Ecology Resources*, 15(6), 1289–1303. <https://doi.org/10.1111/1755-0998.12402>
- Siegfried, C. A., & Kopache, M. E. (1980). Feeding of *Neomysis mercedis* (Holmes). *The Biological Bulletin*, 159, 193–205. <https://doi.org/10.2307/1541018>
- Shimomura, M., Ohtsuka, S., & Naito, K. (2005). *Prodajus curviabdominalis* n. sp. (Isopoda: Epicaridea: Dajidae), an ectoparasite of mysids, with notes on morphological changes, behaviour and life-cycle. *Systematic Parasitology*, 60, 39–57.
<https://doi.org/10.1007/s11230-004-1375-8>
- Schoch, C. L., Seifert, K. A., Huhndorf, S., Robert, V., Spouge, J. L., Levesque, C. A., Chen, W., & Consortium, F. B. (2012). Nuclear ribosomal internal transcribed spacer (ITS) region as a universal DNA barcode marker for Fungi. *Proceedings of the National Academy of Sciences - PNAS*, 109, 6241–6246. <https://doi.org/10.1073/pnas.1117018109>

- Taberlet, P., Coissac, E., Pompanon, F., Brochmann, C., & Willerslev, E. (2012). Towards next-generation biodiversity assessment using DNA metabarcoding. *Molecular Ecology*, *21*, 2045–2050. <https://doi.org/10.1111/j.1365-294X.2012.05470.x>
- Takahashi, K., Nagao, N., & Taguchi, S. (2015). Diel distribution and feeding habits of *Neomysis mirabilis* under seasonal sea ice in a subarctic lagoon of northern Japan. *Aquatic Biology*, *23*, 183–190. <https://doi.org/10.3354/ab00620>
- Viitasalo, M., & Rautio, M. (1998). Zooplanktivory by *Praunus flexuosus* (Crustacea: Mysidacea): functional responses and prey selection in relation to prey escape responses. *Marine Ecology. Progress Series (Halstenbek)*, *174*, 77–87. <https://doi.org/10.3354/meps174077>
- Wilhelm, F. M., Hamann, J., & Burns, C. W. (2002). Mysid predation on amphipods and *Daphnia* in a shallow coastal lake: prey selection and effects of macrophytes. *Canadian Journal of Fisheries and Aquatic Sciences*, *59*, 1901–1907. <https://doi.org/10.1139/f02-161>
- Winkler, G., Martineau, C., Dodson, J. J., Vincent, W. F., & Johnson, L. E. (2007). Trophic dynamics of two sympatric mysid species in an estuarine transition zone. *Marine Ecology Progress Series*, *332*, 171–187. <https://doi.org/10.3354/meps332171>
- Wood S.N. (2011). “Fast stable restricted maximum likelihood and marginal likelihood estimation of semiparametric generalized linear models.” *Journal of the Royal Statistical Society (B)*, *73*, 3–36. [doi:10.1111/j.1467-9868.2010.00749.x](https://doi.org/10.1111/j.1467-9868.2010.00749.x).
- Yeh, H. D., Questel, J. M., Maas, K. R., & Bucklin, A. (2020). Metabarcoding analysis of regional variation in gut contents of the copepod *Calanus finmarchicus* in the North

Atlantic Ocean. *Deep Sea Research Part II: Topical Studies in Oceanography*, 180, 104738-. <https://doi.org/10.1016/j.dsr2.2020.104738>

Zagursky, G., & Feller, R. J. (1985). Macrophyte Detritus in the Winter Diet of the Estuarine Mysid, *Neomysis americana*. *Estuaries*, 8, 355–362. <https://doi.org/10.2307/1351873>

Zamora-Terol, S., Novotny, A., & Winder, M. (2020). Reconstructing marine plankton food web interactions using DNA metabarcoding. *Molecular Ecology*, 29, 3380–3395. <https://doi.org/10.1111/mec.15555>

Appendix A

Tables

Table A1.1: Number of fish caught by species in beach seine sampling per day. See Table 1.3 for species name abbreviations.

Date Caught	Fish Species										
	AC	AN	BD	HB	AM	SK	SP	ST	SS	WF	WP
8/15/23	3	0	0	0	0	0	0	2	0	0	1
8/31/23	1	28	0	9	0	0	2	0	1	1	0
9/15/23	2	27	0	1	0	0	5	3	0	0	0
9/18/23	4	12	1	1	0	2	3	3	0	0	0
9/28/23	2	14	0	0	3	0	0	0	0	0	4

Table A1.2: Correlation coefficients between fish and mysid abundances (upper diagonal) and p-values of the correlations between fish and mysid abundances (lower diagonal). See Table 1.3 for species name abbreviations.

Species	AC	AN	SK	SP	ST	WF	WP	Mysids
AC	NA	-0.6861	0.784	0.00	0.694	-0.686	-0.127	-0.391
AN	0.201	NA	-0.202	0.659	-0.179	0.567	-0.310	0.079
SK	0.116	0.745	NA	0.264	0.516	-0.250	-0.323	-0.305
SP	1.00	0.227	0.668	NA	0.622	0.00	-0.680	-0.187
ST	0.194	0.774	0.373	0.263	NA	-0.590	-0.571	-0.310
WF	0.201	0.319	0.685	1.00	0.295	NA	-0.322	0.776
WP	0.839	0.611	0.596	0.206	0.315	0.596	NA	-0.473
Mysids	0.515	0.899	0.617	0.763	0.611	0.123	0.421	NA

Table A1.3: Relative variability of the daily mysid mortality rates by fish species. See Table 1.3 for species name abbreviations.

Species	Relative Variability
AC	0.871
AN	0.953
SP	0.611
SK	0.948
ST	0.938
WF	0.937
WP	0.964

Table A2.1. Sample information from collections from the St. Marys River (SMR) and Patuxent River (PAX), Maryland. Information includes sample identification number (Sample #), the river of collection, the date and time collected, site within the rivers, and the mean mysid length of the sample (average of 4 individual mysid lengths). For the Patuxent River sampling, the water column position (“Midwater” or “Surface”), and categorical time of day factor (“Night” for the 9:00 PM and 11:30 PM samples, and “Morning” for the 1:30 AM and 3:00 AM samples) are also included.

Sample #	River	Date	Time	Site	Mysid Length (mm)	Water Column	Time of Night
001	SMR	04/10/24	01:00 PM	2	6.84	–	–
002	SMR	04/10/24	01:00 PM	2	6.50	–	–
003	SMR	04/10/24	01:00 PM	2	5.55	–	–
004	SMR	04/10/24	01:00 PM	2	4.97	–	–
005	SMR	04/10/24	01:00 PM	2	4.72	–	–
006	SMR	04/10/24	10:00 AM	1	6.38	–	–
007	SMR	04/10/24	10:00 AM	1	5.59	–	–
008	SMR	04/10/24	10:00 AM	1	3.70	–	–
009	SMR	04/10/24	10:00 AM	1	6.34	–	–
010	SMR	04/10/24	10:00 AM	1	5.97	–	–
021	PAX	05/16/24	09:00 PM	2	5.49	Surface	Night
022	PAX	05/16/24	09:00 PM	2	4.66	Surface	Night
023	PAX	05/16/24	09:00 PM	2	4.90	Surface	Night
024	PAX	05/16/24	09:00 PM	2	6.65	Surface	Night
025	PAX	05/16/24	09:00 PM	2	6.38	Surface	Night
026	PAX	05/16/24	09:00 PM	2	5.14	Surface	Night
027	PAX	05/16/24	09:00 PM	2	5.49	Surface	Night
028	PAX	05/16/24	09:00 PM	2	5.49	Surface	Night
029	PAX	05/16/24	09:00 PM	2	7.50	Surface	Night
030	PAX	05/16/24	09:00 PM	2	3.63	Surface	Night

031	PAX	05/16/24	09:00 PM	2	3.85	Midwater	Night
034	PAX	05/16/24	09:00 PM	2	8.45	Midwater	Night
035	PAX	05/16/24	09:00 PM	2	7.71	Midwater	Night
036	PAX	05/16/24	09:00 PM	2	7.96	Midwater	Night
037	PAX	05/16/24	09:00 PM	2	8.38	Midwater	Night
038	PAX	05/16/24	09:00 PM	2	9.29	Midwater	Night
039	PAX	05/16/24	09:00 PM	2	8.73	Midwater	Night
040	PAX	05/16/24	09:00 PM	2	9.42	Midwater	Night
041	PAX	05/16/24	09:00 PM	2	9.45	Midwater	Night
042	PAX	05/16/24	09:00 PM	2	9.05	Midwater	Night
043	PAX	05/16/24	09:00 PM	2	10.17	Midwater	Night
044	PAX	05/16/24	11:30 PM	5	4.57	Surface	Night
045	PAX	05/16/24	11:30 PM	5	5.44	Surface	Night
046	PAX	05/16/24	11:30 PM	5	6.13	Surface	Night
047	PAX	05/16/24	11:30 PM	5	8.21	Surface	Night
048	PAX	05/16/24	11:30 PM	5	8.26	Surface	Night
049	PAX	05/16/24	11:30 PM	5	4.55	Surface	Night
050	PAX	05/16/24	11:30 PM	5	7.85	Surface	Night
051	PAX	05/16/24	11:30 PM	5	4.20	Surface	Night
052	PAX	05/16/24	11:30 PM	5	7.49	Surface	Night
053	PAX	05/16/24	11:30 PM	5	9.40	Surface	Night
054	PAX	05/16/24	11:30 PM	5	4.47	Midwater	Night
055	PAX	05/16/24	11:30 PM	5	4.52	Midwater	Night
056	PAX	05/16/24	11:30 PM	5	3.90	Midwater	Night
057	PAX	05/16/24	11:30 PM	5	4.28	Midwater	Night

058	PAX	05/16/24	11:30 PM	5	4.66	Midwater	Night
059	PAX	05/16/24	11:30 PM	5	4.39	Midwater	Night
060	PAX	05/16/24	11:30 PM	5	5.47	Midwater	Night
061	PAX	05/16/24	11:30 PM	5	7.12	Midwater	Night
062	PAX	05/16/24	11:30 PM	5	8.44	Midwater	Night
063	PAX	05/16/24	11:30 PM	5	8.51	Midwater	Night
064	PAX	05/17/24	01:30 AM	2	2.90	Surface	Morning
065	PAX	05/17/24	01:30 AM	2	2.87	Surface	Morning
066	PAX	05/17/24	01:30 AM	2	2.49	Surface	Morning
067	PAX	05/17/24	01:30 AM	2	4.05	Surface	Morning
068	PAX	05/17/24	01:30 AM	2	3.70	Surface	Morning
069	PAX	05/17/24	01:30 AM	2	4.12	Surface	Morning
070	PAX	05/17/24	01:30 AM	2	5.54	Surface	Morning
071	PAX	05/17/24	01:30 AM	2	5.59	Surface	Morning
072	PAX	05/17/24	01:30 AM	2	6.62	Surface	Morning
073	PAX	05/17/24	01:30 AM	2	6.25	Midwater	Morning
074	PAX	05/17/24	01:30 AM	2	4.74	Midwater	Morning
075	PAX	05/17/24	01:30 AM	2	6.00	Midwater	Morning
076	PAX	05/17/24	01:30 AM	2	8.96	Midwater	Morning
077	PAX	05/17/24	01:30 AM	2	9.09	Midwater	Morning
078	PAX	05/17/24	01:30 AM	2	10.32	Midwater	Morning
079	PAX	05/17/24	01:30 AM	2	4.18	Midwater	Morning
080	PAX	05/17/24	01:30 AM	2	3.90	Midwater	Morning
081	PAX	05/17/24	01:30 AM	2	6.26	Midwater	Morning
082	PAX	05/17/24	01:30 AM	2	9.14	Midwater	Morning

083	PAX	05/17/24	01:30 AM	2	8.83	Midwater	Morning
084	PAX	05/17/24	03:00 AM	5	5.62	Midwater	Morning
085	PAX	05/17/24	03:00 AM	5	6.84	Midwater	Morning
086	PAX	05/17/24	03:00 AM	5	4.54	Midwater	Morning
087	PAX	05/17/24	03:00 AM	5	8.41	Midwater	Morning
088	PAX	05/17/24	03:00 AM	5	3.85	Midwater	Morning
089	PAX	05/17/24	03:00 AM	5	4.49	Midwater	Morning
090	PAX	05/17/24	03:00 AM	5	4.61	Midwater	Morning
091	PAX	05/17/24	03:00 AM	5	4.44	Midwater	Morning
092	PAX	05/17/24	03:00 AM	5	5.11	Midwater	Morning
093	PAX	05/17/24	03:00 AM	5	6.29	Midwater	Morning
094	PAX	05/17/24	03:00 AM	5	4.99	Surface	Morning
095	PAX	05/17/24	03:00 AM	5	4.76	Surface	Morning
096	PAX	05/17/24	03:00 AM	5	5.19	Surface	Morning
097	PAX	05/17/24	03:00 AM	5	6.01	Surface	Morning
098	PAX	05/17/24	03:00 AM	5	5.46	Surface	Morning
099	PAX	05/17/24	03:00 AM	5	7.06	Surface	Morning
100	PAX	05/17/24	03:00 AM	5	4.34	Surface	Morning
101	PAX	05/17/24	03:00 AM	5	3.81	Surface	Morning
102	PAX	05/17/24	03:00 AM	5	3.57	Surface	Morning
103	PAX	05/17/24	03:00 AM	5	3.44	Surface	Morning

Table A2.2. Model information for generalized additive models of the abundance of sequences in the stomachs of St. Marys mysid-excluded samples. The columns are designated by the intercept (Int), factors (Mysid Length (L), Site, degrees of freedom (df), logLikelihood (LL), AICc, delta, and weight.

Int	L (mm)	Site	df	LL	AICc	delta	weight
9.120	NA	+	3	-160.802	328.695	0.000	0.460
8.293	+	+	4	-159.564	329.036	0.341	0.388
5.851	+	NA	3	-162.065	331.226	2.531	0.130
6.227	NA	NA	2	-165.135	334.792	6.098	0.022

Table A2.3. Model information for generalized additive models of the abundance of sequences in the stomachs of St. Marys mysid-included samples. The column headers are as designated in A2.2.

Int	L (mm)	Site	df	LL	AICc	delta	weight
9.830	NA	NA	2	-353.874	712.064	0.000	0.562
9.812	+	NA	3	-353.742	714.135	2.071	0.200
9.528	NA	+	2	-353.844	714.337	2.273	0.180
9.626	+	+	4	-353.746	716.605	4.541	0.058

Table A2.4. Model information for generalized additive models of the presence of sequences in the stomachs of Patuxent mysid-excluded samples. The variables are for length of the consumer mysid (*L*(mm)), site the sample came from (*Site*), time of night sampled (*Time*), and the water column position (*WC*).

Int	L (mm)	Site	Time	WC	df	LL	AICc	delta	weight
-5.788	0.691	NA	NA	NA	2	-33.038	70.230	0.000	0.2925
-6.733	0.768	+	NA	NA	3	-32.297	70.906	0.676	0.2085
-5.199	0.639	NA	NA	+	3	-32.710	71.732	1.502	0.1380
-6.230	0.725	+	NA	+	4	-31.829	72.185	1.955	0.1100
-5.793	0.689	NA	+	NA	3	-33.037	72.385	2.155	0.0996
-6.733	0.769	+	+	NA	4	-32.297	73.121	2.891	0.0689
-5.192	0.628	NA	+	+	4	-32.688	73.902	3.672	0.0466
-6.225	0.718	+	+	+	5	-31.819	74.439	4.209	0.0356
-0.619	NA	NA	NA	+	2	-41.100	86.355	16.125	0.0000
-1.009	NA	NA	+	+	3	-40.208	86.729	16.499	0.0000
-0.555	NA	+	NA	+	3	-41.072	88.455	18.225	0.0000
-0.946	NA	+	+	+	4	-40.182	88.889	18.659	0.0000
-1.183	NA	NA	NA	NA	1	-44.124	90.298	20.068	0.0000
-1.551	NA	NA	+	NA	2	-43.335	90.824	20.594	0.0000
-1.131	NA	+	NA	NA	2	-44.104	92.361	22.131	0.0000
-1.502	NA	+	+	NA	3	-43.318	92.947	22.717	0.0000

Table A2.5. Model information for generalized additive models of the abundance of sequences in the stomachs of Patuxent mysid-excluded samples. The column headers are as designated in A2.4.

Int	L (mm)	Site	Time	WC	df	LL	AICc	delta	weight
5.161	+	NA	+	NA	4	-285.448	579.314	0.000	0.297
5.139	+	+	+	NA	5	-284.660	579.949	0.635	0.216
3.559	+	NA	NA	NA	3	-287.205	580.660	1.346	0.151
5.101	+	NA	+	+	5	-285.413	581.456	2.142	0.102
5.259	+	+	+	+	6	-284.414	581.716	2.401	0.089
3.720	+	NA	NA	+	4	-287.104	582.625	3.311	0.057
3.514	+	+	NA	NA	4	-287.217	582.850	3.536	0.051
3.566	+	+	NA	+	5	-286.638	583.904	4.590	0.030
2.619	NA	NA	+	NA	3	-291.078	588.401	9.087	0.003
2.704	NA	NA	+	+	4	-290.541	589.495	10.181	0.002
2.726	NA	+	+	NA	4	-290.957	590.326	11.012	0.001
2.567	NA	+	+	+	5	-290.279	591.183	11.869	0.001
4.553	NA	NA	NA	NA	2	-295.073	594.266	14.952	0.000
4.519	NA	+	NA	NA	3	-295.080	596.405	17.091	0.000
4.526	NA	NA	NA	+	3	-295.081	596.408	17.093	0.000
4.519	NA	+	NA	+	4	-295.098	598.609	19.294	0.000

Table A2.6. Table of the model selection for which factors best predicted abundance of sequences in the stomachs of Patuxent mysid-included samples. The column headers are as designated in A2.4.

Int	L (mm)	Site	Time	WC	df	LL	AICc	delta	weight
5.677	+	NA	+	+	11	-530.670	1088.364	0.000	0.587
5.111	+	NA	NA	+	10	-533.441	1090.396	2.033	0.213
5.443	+	+	+	+	12	-530.893	1091.521	3.158	0.121
4.822	+	+	NA	+	11	-533.261	1092.399	4.035	0.078
6.661	+	NA	+	NA	10	-539.064	1103.238	14.874	0.000
6.273	+	NA	NA	NA	9	-540.782	1103.359	14.995	0.000
5.706	+	+	NA	NA	10	-540.829	1105.384	17.020	0.000
6.087	+	+	+	NA	11	-539.994	1106.399	18.035	0.000
7.040	NA	NA	+	+	4	-552.727	1113.974	25.610	0.000
6.643	NA	+	+	+	5	-551.745	1114.279	25.915	0.000
7.363	NA	+	+	NA	4	-556.800	1122.119	33.755	0.000
5.602	NA	+	NA	+	4	-558.299	1125.118	36.755	0.000
6.333	NA	NA	NA	+	2	-561.813	1129.935	41.571	0.000
8.376	NA	NA	+	NA	2	-562.935	1132.179	43.815	0.000
6.706	NA	+	NA	NA	3	-565.900	1138.109	49.745	0.000
7.643	NA	NA	NA	NA	2	-570.038	1144.227	55.863	0.000

Figures

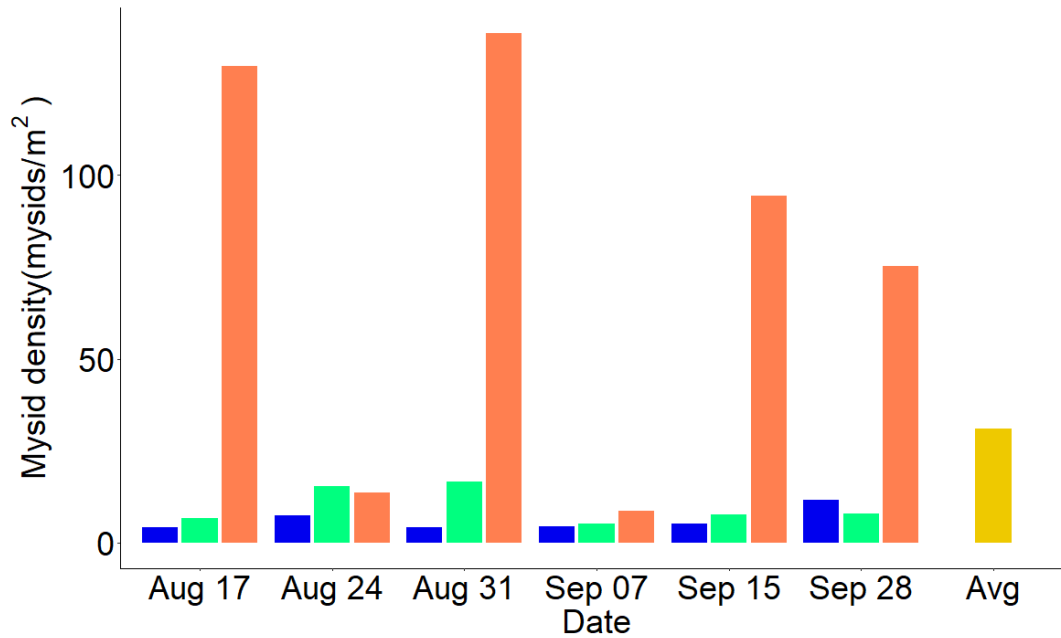


Figure A1.1: Estimated densities of mysids by sampling date and location and average density across all sampling dates and locations (Avg). See Figure 1.1 for locations of sled tows. The density of mysids caught in the structured shallow water habitat (orange) was significantly different than the shallow open (green) water and deep tow (blue) transects (ANOVA; $p = .002$).

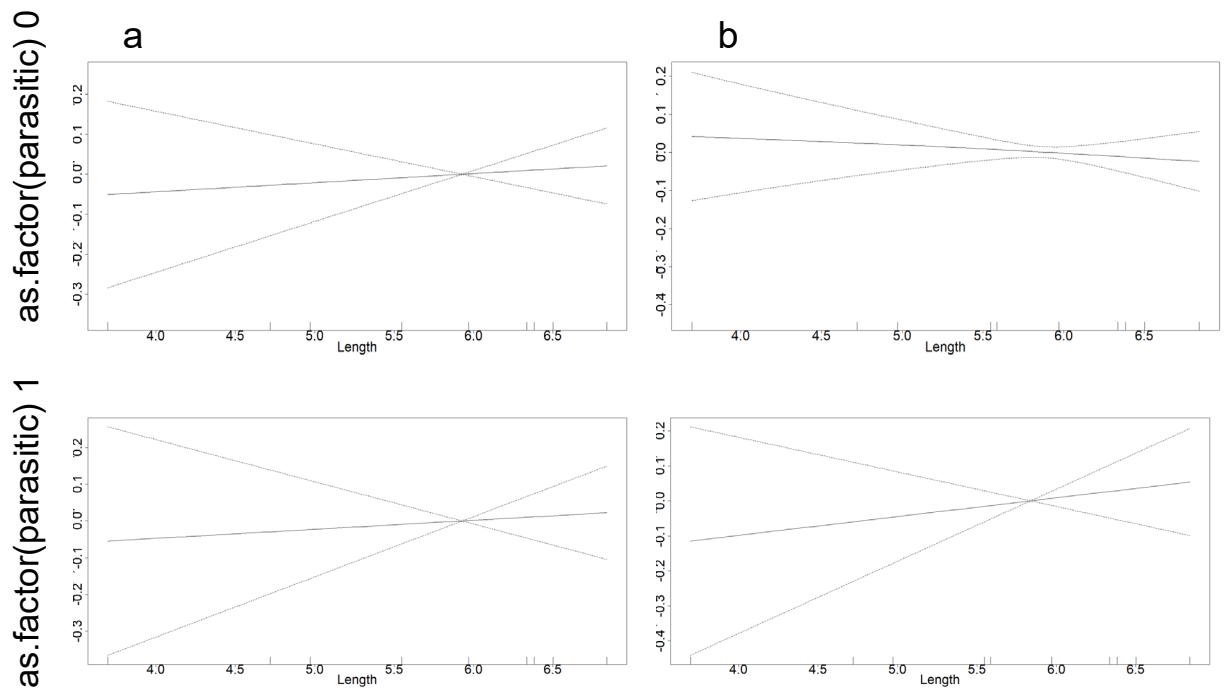


Figure A2.7. Relationship between the length of mysids and the length of the young putative prey with an interaction by parasitism for the St. Marys River a) mysid-excluded and b) mysid-included samples. The top plots represent the samples where parasites were not associated with the sequence, and the bottom plots are samples that had sequences that may be parasites. The solid black lines are the estimated smoothed values and the dashed lines are 95% confidence intervals.

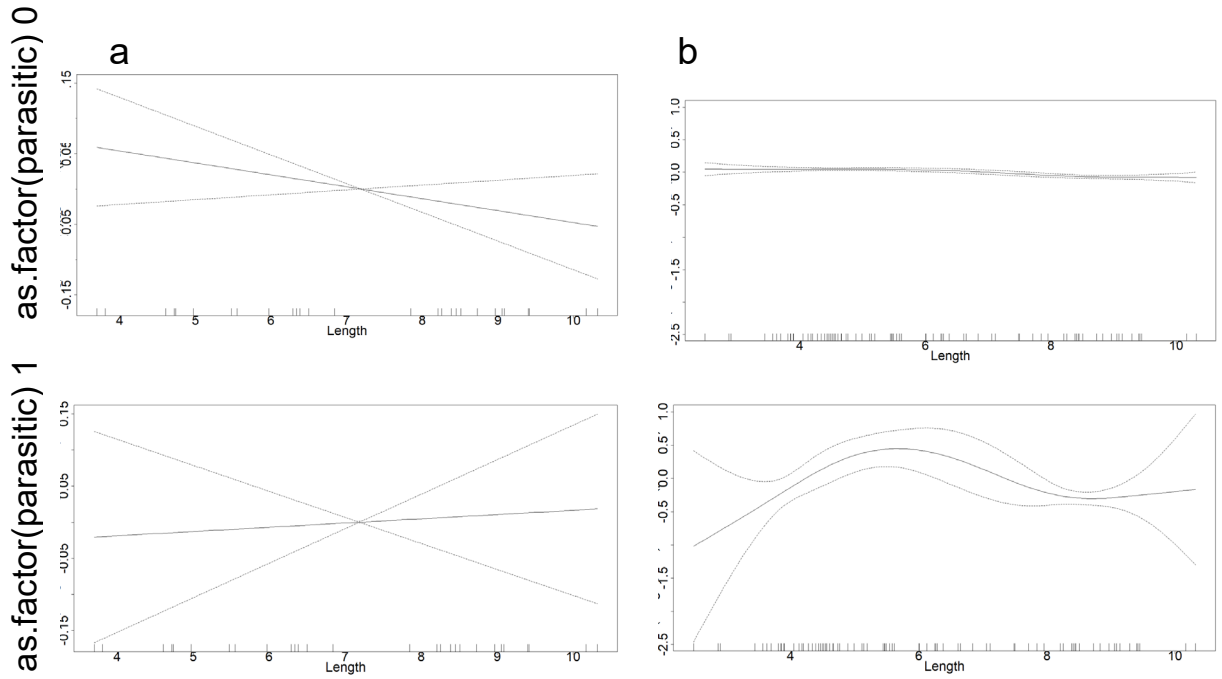


Figure A2.8. Relationship between the length of mysids and the length of the young putative prey with an interaction by parasitism for the Patuxent River a) mysid-excluded and b) mysid-included samples. The top plots represent the samples where parasites were not associated with the sequence, and the bottom plots are samples that had sequences that may be parasites. The solid black lines are the estimated smoothed values and the dashed lines are 95% confidence intervals.

Supplementary Files

File S1. Sources used in the literature review of putative prey identifications. Click to download.
<https://acrobat.adobe.com/id/urn:aaid:sc:VA6C2:0ecca713-0da2-427b-856f-7680b3413051>

